Different FEM approaches for the forward problem in MEG/EEG

Carsten Wolters

Institut für Biomagnetismus und Biosignalanalyse, Westf. Wilhelms-Universität Münster, Germany

outline

- general introduction
- continuous Galerkin for EEG and MEG
- discontinuous Galerkin for EEG and MEG
- unfitted discontinuous Galerkin for EEG
- summary

outline

- general introduction
- continuous Galerkin for EEG and MEG
- discontinuous Galerkin for EEG and MEG
- unfitted discontinuous Galerkin for EEG
- summary

introduction

- electroencephalography (EEG) and magnetoencephalography (MEG) are techniques used to investigate brain activity, with a unique time resolution

introduction

- electroencephalography (EEG) and magnetoencephalography (MEG) are techniques used to investigate brain activity, with a unique time resolution
- EEG $\rightarrow$ electric potential distribution

introduction

- electroencephalography (EEG) and magnetoencephalography (MEG) are techniques used to investigate brain activity, with a unique time resolution
- EEG $\rightarrow$ electric potential distribution
- MEG $\rightarrow$ magnetic field

- electroencephalography (EEG) and magnetoencephalography (MEG) are techniques used to investigate brain activity, with a unique time resolution
- EEG $\rightarrow$ electric potential distribution
- MEG $\rightarrow$ magnetic field
- even if generated by the same sources, MEG and EEG signals differ and carry complementary information

introduction

- electroencephalography (EEG) and magnetoencephalography (MEG) are techniques used to investigate brain activity, with a unique time resolution
- EEG $\rightarrow$ electric potential distribution
- MEG $\rightarrow$ magnetic field
- even if generated by the same sources, MEG and EEG signals differ and carry complementary information
- source reconstruction is an important procedure in many applications

introduction

- electroencephalography (EEG) and magnetoencephalography (MEG) are techniques used to investigate brain activity, with a unique time resolution
- EEG $\rightarrow$ electric potential distribution
- MEG $\rightarrow$ magnetic field
- even if generated by the same sources, MEG and EEG signals differ and carry complementary information
- source reconstruction is an important procedure in many applications
- combined EEG and MEG complementary information provides outperforming source reconstructions in presurgical epilepsy diagnosis

introduction

- electroencephalography (EEG) and magnetoencephalography (MEG) are techniques used to investigate brain activity, with a unique time resolution
- EEG $\rightarrow$ electric potential distribution
- MEG $\rightarrow$ magnetic field
- even if generated by the same sources, MEG and EEG signals differ and carry complementary information
- source reconstruction is an important procedure in many applications
- combined EEG and MEG complementary information provides outperforming source reconstructions in presurgical epilepsy diagnosis

forward problem in EEG and MEG

forward problem in EEG and MEG

- solving the EEG forward problem means solving a partial differential equation

forward problem in EEG and MEG

- solving the EEG forward problem means solving a partial differential equation
- solving the MEG forward problem needs the EEG forward problem solution and it consists in solving an integration problem

forward problem in EEG and MEG

- solving the EEG forward problem means solving a partial differential equation
- solving the MEG forward problem needs the EEG forward problem solution and it consists in solving an integration problem

EEG Forward Problem

the goal is to evaluate the electric potential u

$$\begin{cases} \nabla \cdot (\sigma \nabla u) = \nabla \cdot \mathbf{j}^p, & \text{in } \Omega \subseteq \mathbb{R}^3 \\ \nabla u \cdot \mathbf{n} = 0 & \text{on } \partial\Omega \end{cases}$$

EEG Forward Problem

the goal is to evaluate the electric potential u

$$\begin{cases} \nabla \cdot (\sigma \nabla u) = \nabla \cdot \mathbf{j}^p, & \text{in } \Omega \subseteq \mathbb{R}^3 \\ \nabla u \cdot \mathbf{n} = 0 & \text{on } \partial\Omega \end{cases}$$

where

EEG Forward Problem

the goal is to evaluate the electric potential u

$$\begin{cases} \nabla \cdot (\sigma \nabla u) = \nabla \cdot \mathbf{j}^p, & \text{in } \Omega \subseteq \mathbb{R}^3 \\ \nabla u \cdot \mathbf{n} = 0 & \text{on } \partial\Omega \end{cases}$$

where

- σ conductivity of the brain

EEG Forward Problem

the goal is to evaluate the electric potential u

$$\begin{cases} \nabla \cdot (\sigma \nabla u) = \nabla \cdot \mathbf{j}^p, & \text{in } \Omega \subseteq \mathbb{R}^3 \\ \nabla u \cdot \mathbf{n} = 0 & \text{on } \partial\Omega \end{cases}$$

where

- σ conductivity of the brain
- $\mathbf{j}^p = \mathbf{M} \cdot \delta_{\mathbf{r}_0}$ dipole source

EEG Forward Problem

the goal is to evaluate the electric potential u

$$\begin{cases} \nabla \cdot (\sigma \nabla u) = \nabla \cdot \mathbf{j}^p, & \text{in } \Omega \subseteq \mathbb{R}^3 \\ \nabla u \cdot \mathbf{n} = 0 & \text{on } \partial\Omega \end{cases}$$

where

- σ conductivity of the brain
- $\mathbf{j}^p = \mathbf{M} \cdot \delta_{\mathbf{r}_0}$ dipole source
    - $\mathbf{M}$ dipole moment;

EEG Forward Problem

the goal is to evaluate the electric potential u

$$\begin{cases} \nabla \cdot (\sigma \nabla u) = \nabla \cdot \mathbf{j}^p, & \text{in } \Omega \subseteq \mathbb{R}^3 \\ \nabla u \cdot \mathbf{n} = 0 & \text{on } \partial\Omega \end{cases}$$

where

- σ conductivity of the brain
- $\mathbf{j}^p = \mathbf{M} \cdot \delta_{\mathbf{r}_0}$ dipole source
    - $\mathbf{M}$ dipole moment;
    - $\delta_{\mathbf{r}_0}$ Dirac delta centered in $\mathbf{r}_0$.

EEG Forward Problem

the goal is to evaluate the electric potential u

$$\begin{cases} \nabla \cdot (\sigma \nabla u) = \nabla \cdot \mathbf{j}^p, & \text{in } \Omega \subseteq \mathbb{R}^3 \\ \nabla u \cdot \mathbf{n} = 0 & \text{on } \partial\Omega \end{cases}$$

where

- σ conductivity of the brain
- $\mathbf{j}^p = \mathbf{M} \cdot \delta_{\mathbf{r}_0}$ dipole source
  - $\mathbf{M}$ dipole moment;
  - $\delta_{\mathbf{r}_0}$ Dirac delta centered in $\mathbf{r}_0$.
- analytical solution in sphere model (de Munck et al., 1988)

EEG Forward Problem

the goal is to evaluate the electric potential u

$$\begin{cases} \nabla \cdot (\sigma \nabla u) = \nabla \cdot \mathbf{j}^p, & \text{in } \Omega \subseteq \mathbb{R}^3 \\ \nabla u \cdot \mathbf{n} = 0 & \text{on } \partial\Omega \end{cases}$$

where

- σ conductivity of the brain
- $\mathbf{j}^p = \mathbf{M} \cdot \delta_{\mathbf{r}_0}$ dipole source
  - $\mathbf{M}$ dipole moment;
  - $\delta_{\mathbf{r}_0}$ Dirac delta centered in $\mathbf{r}_0$.
- analytical solution in sphere model (de Munck et al., 1988)
- numerical solution in realistic models

MEG Forward Problem

the goal is to evaluate the magnetic B-field **B** (Biot-Savart):

MEG Forward Problem

the goal is to evaluate the magnetic B-field $\mathbf{B}$ (Biot-Savart):

$$\mathbf{B}(\mathbf{r}) = \frac{\mu_0}{4\pi} \int_\Omega \mathbf{j}(\mathbf{r}') \times \frac{\mathbf{r} - \mathbf{r}'}{|\mathbf{r} - \mathbf{r}'|^3} \, d^3\mathbf{r}'$$

MEG Forward Problem

the goal is to evaluate the magnetic B-field $\mathbf{B}$ (Biot-Savart):

$$\begin{aligned}
\mathbf{B}(\mathbf{r}) &= \frac{\mu_0}{4\pi}\int_\Omega \mathbf{j}(\mathbf{r}') \times \frac{\mathbf{r}-\mathbf{r}'}{|\mathbf{r}-\mathbf{r}'|^3}\, d^3\mathbf{r}' \\
&= \frac{\mu_0}{4\pi}\int_\Omega \underbrace{\left(\mathbf{j}^p(\mathbf{r}') + \mathbf{j}^s(\mathbf{r}')\right)}_{\text{electric current density}} \times \frac{\mathbf{r}-\mathbf{r}'}{|\mathbf{r}-\mathbf{r}'|^3}\, d^3\mathbf{r}'
\end{aligned}$$

MEG Forward Problem

the goal is to evaluate the magnetic B-field **B** (Biot-Savart):

$$
\begin{aligned}
\mathbf{B}(\mathbf{r}) &= \frac{\mu_0}{4\pi}\int_\Omega \mathbf{j}(\mathbf{r}') \times \frac{\mathbf{r}-\mathbf{r}'}{|\mathbf{r}-\mathbf{r}'|^3}\, d^3\mathbf{r}' \\
&= \frac{\mu_0}{4\pi}\int_\Omega \underbrace{\left(\mathbf{j}^p(\mathbf{r}') + \mathbf{j}^s(\mathbf{r}')\right)}_{\text{electric current density}} \times \frac{\mathbf{r}-\mathbf{r}'}{|\mathbf{r}-\mathbf{r}'|^3}\, d^3\mathbf{r}' \\
&= \frac{\mu_0}{4\pi}\mathbf{M} \times \frac{\mathbf{r}-\mathbf{r}_0}{|\mathbf{r}-\mathbf{r}_0|^3} + \frac{\mu_0}{4\pi}\int_\Omega \mathbf{j}^s(\mathbf{r}') \times \frac{\mathbf{r}-\mathbf{r}'}{|\mathbf{r}-\mathbf{r}'|^3}\, d^3\mathbf{r}'
\end{aligned}
$$

MEG Forward Problem

the goal is to evaluate the magnetic B-field **B** (Biot-Savart):

$$
\begin{aligned}
\mathbf{B}(\mathbf{r}) &= \frac{\mu_0}{4\pi} \int_\Omega \mathbf{j}(\mathbf{r}') \times \frac{\mathbf{r}-\mathbf{r}'}{|\mathbf{r}-\mathbf{r}'|^3}\, d^3\mathbf{r}' \\
&= \frac{\mu_0}{4\pi} \int_\Omega \underbrace{\left(\mathbf{j}^p(\mathbf{r}') + \mathbf{j}^s(\mathbf{r}')\right)}_{\text{electric current density}} \times \frac{\mathbf{r}-\mathbf{r}'}{|\mathbf{r}-\mathbf{r}'|^3}\, d^3\mathbf{r}' \\
&= \frac{\mu_0}{4\pi} \mathbf{M} \times \frac{\mathbf{r}-\mathbf{r}_0}{|\mathbf{r}-\mathbf{r}_0|^3} + \frac{\mu_0}{4\pi} \int_\Omega \mathbf{j}^s(\mathbf{r}') \times \frac{\mathbf{r}-\mathbf{r}'}{|\mathbf{r}-\mathbf{r}'|^3}\, d^3\mathbf{r}' \\
&= \mathbf{B}^p(\mathbf{r}) + \mathbf{B}^s(\mathbf{r})
\end{aligned}
$$

MEG Forward Problem

the goal is to evaluate the magnetic B-field **B** (Biot-Savart):

$$
\begin{aligned}
\mathbf{B}(\mathbf{r}) &= \frac{\mu_0}{4\pi} \int_\Omega \mathbf{j}(\mathbf{r}') \times \frac{\mathbf{r} - \mathbf{r}'}{|\mathbf{r} - \mathbf{r}'|^3}\, d^3\mathbf{r}' \\
&= \frac{\mu_0}{4\pi} \int_\Omega \underbrace{\left(\mathbf{j}^p(\mathbf{r}') + \mathbf{j}^s(\mathbf{r}')\right)}_{\text{electric current density}} \times \frac{\mathbf{r} - \mathbf{r}'}{|\mathbf{r} - \mathbf{r}'|^3}\, d^3\mathbf{r}' \\
&= \frac{\mu_0}{4\pi} \mathbf{M} \times \frac{\mathbf{r} - \mathbf{r}_0}{|\mathbf{r} - \mathbf{r}_0|^3} + \frac{\mu_0}{4\pi} \int_\Omega \mathbf{j}^s(\mathbf{r}') \times \frac{\mathbf{r} - \mathbf{r}'}{|\mathbf{r} - \mathbf{r}'|^3}\, d^3\mathbf{r}' \\
&= \mathbf{B}^p(\mathbf{r}) + \mathbf{B}^s(\mathbf{r})
\end{aligned}
$$

MEG Forward Problem

the goal is to evaluate the magnetic B-field **B** (Biot-Savart):

$$
\begin{aligned}
\mathbf{B}(\mathbf{r}) &= \frac{\mu_0}{4\pi}\int_\Omega \mathbf{j}(\mathbf{r}') \times \frac{\mathbf{r}-\mathbf{r}'}{|\mathbf{r}-\mathbf{r}'|^3}\, d^3\mathbf{r}' \\
&= \frac{\mu_0}{4\pi}\int_\Omega \underbrace{\left(\mathbf{j}^p(\mathbf{r}') + \mathbf{j}^s(\mathbf{r}')\right)}_{\text{electric current density}} \times \frac{\mathbf{r}-\mathbf{r}'}{|\mathbf{r}-\mathbf{r}'|^3}\, d^3\mathbf{r}' \\
&= \frac{\mu_0}{4\pi}\mathbf{M} \times \frac{\mathbf{r}-\mathbf{r}_0}{|\mathbf{r}-\mathbf{r}_0|^3} + \frac{\mu_0}{4\pi}\int_\Omega \mathbf{j}^s(\mathbf{r}') \times \frac{\mathbf{r}-\mathbf{r}'}{|\mathbf{r}-\mathbf{r}'|^3}\, d^3\mathbf{r}' \\
&= \mathbf{B}^p(\mathbf{r}) + \mathbf{B}^s(\mathbf{r})
\end{aligned}
$$

where $\mathbf{j}^s$ depends on the EEG forward solution u

MEG Forward Problem

the goal is to evaluate the magnetic flux Φ

$$\Phi = \int_S \mathbf{B} \cdot d\mathbf{s} = \int_S (\nabla \times \mathbf{A}) \cdot d\mathbf{s} = \oint_{C=\partial S} \mathbf{A} \cdot d\mathbf{c}$$

MEG Forward Problem

the goal is to evaluate the magnetic flux Φ

$$\Phi = \int_S \mathbf{B} \cdot d\mathbf{s} = \int_S (\nabla \times \mathbf{A}) \cdot d\mathbf{s} = \oint_{C=\partial S} \mathbf{A} \cdot d\mathbf{c}$$

where

MEG Forward Problem

the goal is to evaluate the magnetic flux Φ

$$\Phi = \int_S \mathbf{B} \cdot d\mathbf{s} = \int_S (\nabla \times \mathbf{A}) \cdot d\mathbf{s} = \oint_{C=\partial S} \mathbf{A} \cdot d\mathbf{c}$$

where

- $\mathbf{B}$ magnetic field

MEG Forward Problem

the goal is to evaluate the magnetic flux Φ

$$\Phi = \int_S \mathbf{B} \cdot d\mathbf{s} = \int_S (\nabla \times \mathbf{A}) \cdot d\mathbf{s} = \oint_{C=\partial S} \mathbf{A} \cdot d\mathbf{c}$$

where

- $\mathbf{B}$ magnetic field
- $\mathbf{A}$ magnetic vector potential

MEG Forward Problem

the goal is to evaluate the magnetic flux Φ

$$\Phi = \int_S \mathbf{B} \cdot d\mathbf{s} = \int_S (\nabla \times \mathbf{A}) \cdot d\mathbf{s} = \oint_{C=\partial S} \mathbf{A} \cdot d\mathbf{c}$$

where

- $\mathbf{B}$ magnetic field
- $\mathbf{A}$ magnetic vector potential
- S face of the sensor

MEG Forward Problem

the goal is to evaluate the magnetic flux Φ

$$\Phi = \int_S \mathbf{B} \cdot d\mathbf{s} = \int_S (\nabla \times \mathbf{A}) \cdot d\mathbf{s} = \oint_{C=\partial S} \mathbf{A} \cdot d\mathbf{c}$$

where

- $\mathbf{B}$ magnetic field
- $\mathbf{A}$ magnetic vector potential
- S face of the sensor
- $C = \partial S$ contour of the coil

MEG Forward Problem

the goal is to evaluate the magnetic flux Φ

$$\Phi = \int_S \mathbf{B} \cdot d\mathbf{s} = \int_S (\nabla \times \mathbf{A}) \cdot d\mathbf{s} = \oint_{C=\partial S} \mathbf{A} \cdot d\mathbf{c}$$

where

- $\mathbf{B}$ magnetic field
- $\mathbf{A}$ magnetic vector potential
- S face of the sensor
- $C = \partial S$ contour of the coil

- analytical solution out of a sphere model (Sarvas, 1987)

MEG Forward Problem

the goal is to evaluate the magnetic flux Φ

$$\Phi = \int_S \mathbf{B} \cdot d\mathbf{s} = \int_S (\nabla \times \mathbf{A}) \cdot d\mathbf{s} = \oint_{C=\partial S} \mathbf{A} \cdot d\mathbf{c}$$

where

- $\mathbf{B}$ magnetic field
- $\mathbf{A}$ magnetic vector potential
- S face of the sensor
- $C = \partial S$ contour of the coil

- analytical solution out of a sphere model (Sarvas, 1987)
- numerical solution once u is computed

forward problem: ingredients

forward problem: ingredients

- head model:
  - electrical features
  - geometrical features

forward problem: ingredients

- head model:
  - electrical features
  - geometrical features

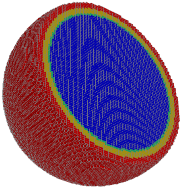

- head model:
  - electrical features
  - geometrical features

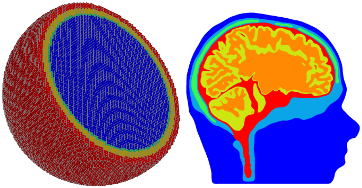

forward problem: ingredients

- head model:
  - electrical features
  - geometrical features

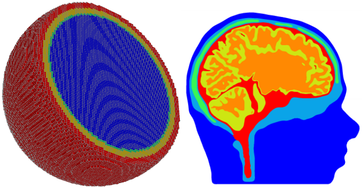

- sensor model

forward problem: ingredients

- head model:
  - electrical features
  - geometrical features

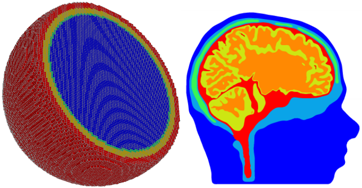

- sensor model
- source model

forward problem: ingredients

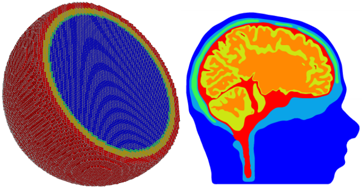

- head model:
  - electrical features
  - geometrical features
- sensor model
- source model
- method:
  - vast spectrum of different numerical methods

head model - 1

head model - 1

Contents lists available at ScienceDirect

NeuroImage

journal homepage: www.elsevier.com/locate/ynimg

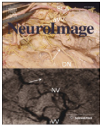

A guideline for head volume conductor modeling in EEG and MEG

Johannes Vorwerk [a,*], Jae-Hyun Cho [b], Stefan Rampp [c], Hajo Hamer [c], Thomas R. Knösche [b], Carsten H. Wolters [a]

[a] Institut für Biomagnetismus und Biosignalanalyse, Westfälische Wilhelms-Universität, Münster, Germany
[b] Max Planck Institute for Human Cognitive and Brain Sciences, Leipzig, Germany
[c] Epilepsiezentrum, Universitätsklinikum Erlangen, Erlangen, Germany

head model - 2

Table 1
Overview of the compartment conductivities, the conductive features of the different head models (I is considered, - is disregarded,: is further divided, and A is anisotropic), and their resolution.

Compartment	σ S/m	*3CI*	*4CI*	*5CI*	*6CI*	*6CA*	*6CA_hr*
Brain	0.33	I	I	:	:	:	:
Brain GM	0.33	-	-	I	I	I	I
Brain WM	0.14	-	-	I	I	A	A
CSF	1.79	-	I	I	I	I	I
Skin	0.43	I	I	I	I	I	I
Skull	0.01	I	I	I	:	:	:
Skull comp.	0.008	-	-	-	I	I	I
Skull spong.	0.025	-	-	-	I	I	I
Resolution	#Nodes	984,569	984,569	984,569	984,569	984,569	2,159,337

head model - 3

- realistic modeling of the volume conductor has strong effects on both EEG and MEG (superficial sources)

head model - 3

- realistic modeling of the volume conductor has strong effects on both EEG and MEG (superficial sources)
- numerical inaccuracies are negligible compared to modeling effects

head model - 3

- realistic modeling of the volume conductor has strong effects on both EEG and MEG (superficial sources)
- numerical inaccuracies are negligible compared to modeling effects
- guideline:

head model - 3

- realistic modeling of the volume conductor has strong effects on both EEG and MEG (superficial sources)
- numerical inaccuracies are negligible compared to modeling effects
- guideline:
    1. CSF

head model - 3

- realistic modeling of the volume conductor has strong effects on both EEG and MEG (superficial sources)
- numerical inaccuracies are negligible compared to modeling effects
- guideline:
  1. CSF
  2. grey/white matter distinction

head model - 3

- realistic modeling of the volume conductor has strong effects on both EEG and MEG (superficial sources)
- numerical inaccuracies are negligible compared to modeling effects
- guideline:
  1. CSF
  2. grey/white matter distinction
  3. white matter anisotropy

head model - 3

- realistic modeling of the volume conductor has strong effects on both EEG and MEG (superficial sources)
- numerical inaccuracies are negligible compared to modeling effects
- guideline:
  1. CSF
  2. grey/white matter distinction
  3. white matter anisotropy
  4. skull compacta/spongiosa

head model - 3

- realistic modeling of the volume conductor has strong effects on both EEG and MEG (superficial sources)
- numerical inaccuracies are negligible compared to modeling effects
- guideline:
  1. CSF
  2. grey/white matter distinction
  3. white matter anisotropy
  4. skull compacta/spongiosa

numerical methods to solve partial differential equations

- Boundary Element Method (BEM)
- Finite Element Method (FEM)
- Finite Volume Method (FVM)
- Finite Difference Method (FDM)

numerical methods

- Boundary Element Method (BEM)
- Finite Element Method (FEM)
  - Continuous Galerkin (CG)
  - Discontinuous Galerkin (DG)
  - Unfitted Discontinuous Galerkin (UDG)
  - Mixed Fomulation
  - Immersed
  - ...
- Finite Volume Method (FVM)
- Finite Difference Method (FDM)

numerical methods

- Boundary Element Method (BEM)

  (Mosher et al., 1999; Kybic et al., 2005; Acar and Makeig, 2010; Gramfort et al., 2011; Stenroos and Sarvas, 2012)
- Finite Element Method (FEM)
  - Continuous Galerkin (CG)

    (Bertrand et al., 1991; Marin et al., 1998; Schimpf et al., 2002; Drechsler et al., 2009; Pursiainen et al., 2016)
  - Discontinuous Galerkin (DG)

    (Engwer et al., 2017)
  - Unfitted Discontinuous Galerkin (UDG)

    (Ning et al., 2016)
  - Mixed Fomulation

    (Vorwerk et al., 2017)
  - Immersed

    (Vallaghé et al., 2008)
  - ...
- Finite Volume Method (FVM)

  (Cook and Koles, 2006)
- Finite Difference Method (FDM)

  (Wendel et al., 2008; Vatta et al., 2009; Montes-Restrepo et al., 2014)

numerical methods

- Boundary Element Method (BEM)
- Finite Element Method (FEM)
  - Continuous Galerkin (CG)
  - Discontinuous Galerkin (DG)
  - Unfitted Discontinuous Galerkin (UDG)
  - Mixed Fomulation
  - Immersed
  - ...
- Finite Volume Method (FVM)
- Finite Difference Method (FDM)

Galerkin method to solve a pde

Strong Formulation

Galerkin method to solve a pde

Strong Formulation

$$\downarrow$$

Galerkin method to solve a pde

Strong Formulation

$$\downarrow$$

Weak (Variational) Formulation

Galerkin method to solve a pde

Strong Formulation

$\downarrow$

Weak (Variational) Formulation

$\downarrow$

Galerkin method to solve a pde

Strong Formulation

$\downarrow$

Weak (Variational) Formulation

$\downarrow$

Discrete Weak (Variational) Formulation

Strong Formulation

↓

Weak Formulation

↓

Discrete Weak Formulation

Strong Formulation

$$?u : \Delta u = f$$

$\downarrow$

Weak Formulation

$\downarrow$

Discrete Weak Formulation

Strong Formulation

$$?u : \Delta u = f$$

$\downarrow$

$\downarrow$

Weak Formulation

$\downarrow$

Discrete Weak Formulation

Strong Formulation

$$?u : \Delta u = f$$

$$\downarrow$$

$\downarrow$

$$?u \in V : \int_{\Omega} (\Delta u = f) v \ d\Omega \ , \forall \ v \in V$$

Weak Formulation

$$?u \in V : \int_{\Omega} \nabla u \nabla v \ d\Omega = \int_{\Omega} fv \ d\Omega \ , \forall \ v \in V$$

$\downarrow$

Discrete Weak Formulation

Strong Formulation

$$?u : \Delta u = f$$

$\downarrow$

$\downarrow$

Weak Formulation

$$?u \in V : \int_\Omega (\Delta u = f) v \; d\Omega \; , \forall \; v \in V$$

$$?u \in V : \int_\Omega \nabla u \nabla v \; d\Omega = \int_\Omega f v \; d\Omega \; , \forall \; v \in V$$

$\downarrow$

$\downarrow$

Discrete Weak Formulation

Strong Formulation

$$?u : \Delta u = f$$

$\downarrow$

$\downarrow$

Weak Formulation

$$?u \in V : \int_\Omega (\Delta u = f) v \; d\Omega \;, \forall \; v \in V$$

$$?u \in V : \int_\Omega \nabla u \nabla v \; d\Omega = \int_\Omega f v \; d\Omega \;, \forall \; v \in V$$

$\downarrow$

$\downarrow$

Discrete Weak Formulation

$$?u_h \in V_h : a(u_h, v_h) = l(v_h) \;, \forall \; v_h \in V_h$$

Strong Formulation

$$?u : \Delta u = f$$

$\downarrow$

$\downarrow$

Weak Formulation

$$?u \in V : \int_\Omega (\Delta u = f) v \; d\Omega \;, \forall \; v \in V$$

$$?u \in V : \int_\Omega \nabla u \nabla v \; d\Omega = \int_\Omega fv \; d\Omega \;, \forall \; v \in V$$

$\downarrow$

$\downarrow$

Discrete Weak Formulation

$$?u_h \in V_h : a(u_h, v_h) = l(v_h) \;, \forall \; v_h \in V_h$$

$$A\mathbf{u} = \mathbf{f}$$

Lagrange-type elements: d.o.f. node-based, shape functions are continuous

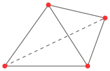

Lagrange-type elements: d.o.f. node-based, shape functions are continuous

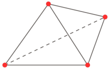

L^2 *- conforming elements*: d.o.f. cell-based, continuity across element interfaces is not required

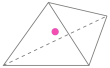

Lagrange-type elements: d.o.f. node-based, shape functions are continuous

CONTINUOUS GALERKIN (CG)

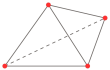

Lagrange-type elements: d.o.f. node-based, shape functions are continuous

CONTINUOUS GALERKIN (CG)

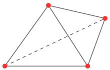

L^2 *- conforming elements*: d.o.f. cell-based, continuity across element interfaces is not required

DISCONTINUOUS GALERKIN (DG)

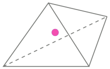

- general introduction
- continuous Galerkin for EEG and MEG
- discontinuous Galerkin for EEG and MEG
- unfitted discontinuous Galerkin for EEG
- summary

CG-FEM and the subtraction approach - EEG

the goal is to evaluate the electric potential u

$$\begin{cases} \nabla \cdot (\sigma \nabla u) = \nabla \cdot \mathbf{j}^p, & \text{in } \Omega \subseteq \mathbb{R}^3 \\ \nabla u \cdot \mathbf{n} = 0 & \text{on } \partial\Omega \end{cases}$$

CG-FEM and the subtraction approach - EEG

the goal is to evaluate the electric potential u

$$\begin{cases} \nabla \cdot (\sigma \nabla u) = \nabla \cdot \mathbf{j}^p, & \text{in } \Omega \subseteq \mathbb{R}^3 \\ \nabla u \cdot \mathbf{n} = 0 & \text{on } \partial\Omega \end{cases}$$

split u and σ

$$u = u^\infty + u^{corr}$$

$$\sigma = \sigma^\infty + \sigma^{corr}$$

where u^∞ is solution of Poisson equation in an unbounded and homogeneous domain with conductivity σ^∞

when multiplying with a test function $v_h \in V_h$ and integrating by parts we obtain the *weak formulation:*

CG-FEM and the subtraction approach - EEG

when multiplying with a test function $v_h \in V_h$ and integrating by parts we obtain the *weak formulation:*

CG - FEM (Drechsler et al., 2009)

find $u_h^{corr} \in V_h \subset H^1$ s.t.

$$\int_\Omega \sigma \nabla u_h^{corr} \cdot \nabla v_h dx = -\int_\Omega \sigma^{corr} \nabla u^\infty \cdot \nabla v_h dx - \int_{\partial\Omega} \sigma^\infty \nabla u^\infty \cdot \mathbf{n} v_h ds)$$

CG-FEM and the subtraction approach - EEG

when multiplying with a test function $v_h \in V_h$ and integrating by parts we obtain the *weak formulation:*

CG - FEM (Drechsler et al., 2009)

find $u_h^{corr} \in V_h \subset H^1$ s.t.

$$\int_\Omega \sigma \nabla u_h^{corr} \cdot \nabla v_h dx = -\int_\Omega \sigma^{corr} \nabla u^\infty \cdot \nabla v_h dx - \int_{\partial\Omega} \sigma^\infty \nabla u^\infty \cdot \mathbf{n} v_h ds)$$

(the solution exists and it is unique)
(derivation of the weak form on the smart board)

CG-FEM and the subtraction approach - MEG

CG-FEM and the subtraction approach - MEG

$$\mathbf{B}(\mathbf{r}) = \mathbf{B}^p(\mathbf{r}) + \mathbf{B}^s(\mathbf{r})$$

$$\mathbf{B}^s(\mathbf{r}) = \frac{\mu_0}{4\pi} \int_\Omega \mathbf{j}^s(\mathbf{r}') \times \frac{\mathbf{r} - \mathbf{r}'}{|\mathbf{r} - \mathbf{r}'|^3} \, d^3\mathbf{r}'$$

CG-FEM and the subtraction approach - MEG

$$\mathbf{B}(\mathbf{r}) = \mathbf{B}^p(\mathbf{r}) + \mathbf{B}^s(\mathbf{r})$$

$$\mathbf{B}^s(\mathbf{r}) = \frac{\mu_0}{4\pi} \int_\Omega \mathbf{j}^s(\mathbf{r}') \times \frac{\mathbf{r} - \mathbf{r}'}{|\mathbf{r} - \mathbf{r}'|^3} \, d^3\mathbf{r}'$$

$$\mathbf{B}^s(\mathbf{r}) = \frac{\mu_0}{4\pi} \int_\Omega \sigma \nabla u(\mathbf{r}') \times \frac{\mathbf{r} - \mathbf{r}'}{|\mathbf{r} - \mathbf{r}'|^3} \, d^3\mathbf{r}'$$

CG-FEM and the subtraction approach - MEG

$$\mathbf{B}(\mathbf{r}) = \mathbf{B}^p(\mathbf{r}) + \mathbf{B}^s(\mathbf{r})$$

$$\mathbf{B}^s(\mathbf{r}) = \frac{\mu_0}{4\pi}\int_\Omega \mathbf{j}^s(\mathbf{r}') \times \frac{\mathbf{r}-\mathbf{r}'}{|\mathbf{r}-\mathbf{r}'|^3}\, d^3\mathbf{r}'$$

$$\mathbf{B}^s(\mathbf{r}) = \frac{\mu_0}{4\pi}\int_\Omega \sigma\nabla u(\mathbf{r}') \times \frac{\mathbf{r}-\mathbf{r}'}{|\mathbf{r}-\mathbf{r}'|^3}\, d^3\mathbf{r}'$$

$$\mathbf{B}^s(\mathbf{r}) = \frac{\mu_0}{4\pi}\int_\Omega (\sigma\nabla u^\infty(\mathbf{r}') + \sigma\nabla u^{corr}(\mathbf{r}')) \times \frac{\mathbf{r}-\mathbf{r}'}{|\mathbf{r}-\mathbf{r}'|^3}\, d^3\mathbf{r}'$$

outline

- general introduction
- continuous Galerkin for EEG and MEG
- discontinuous Galerkin for EEG and MEG
- unfitted discontinuous Galerkin for EEG
- summary

the Discontinuous Galerkin method in **EEG**

[Engwer et al., SIAM J. Scientific Comp., 2017]

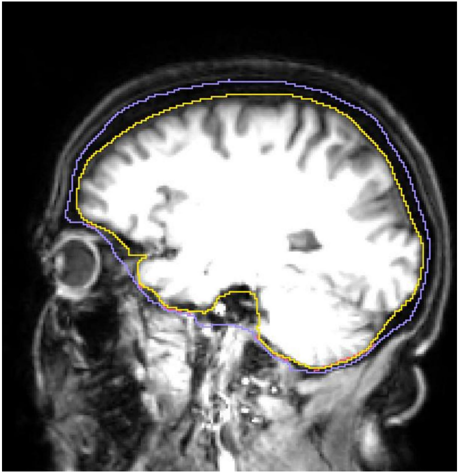

the Discontinuous Galerkin method in **EEG**

[Engwer et al., SIAM J. Scientific Comp., 2017]

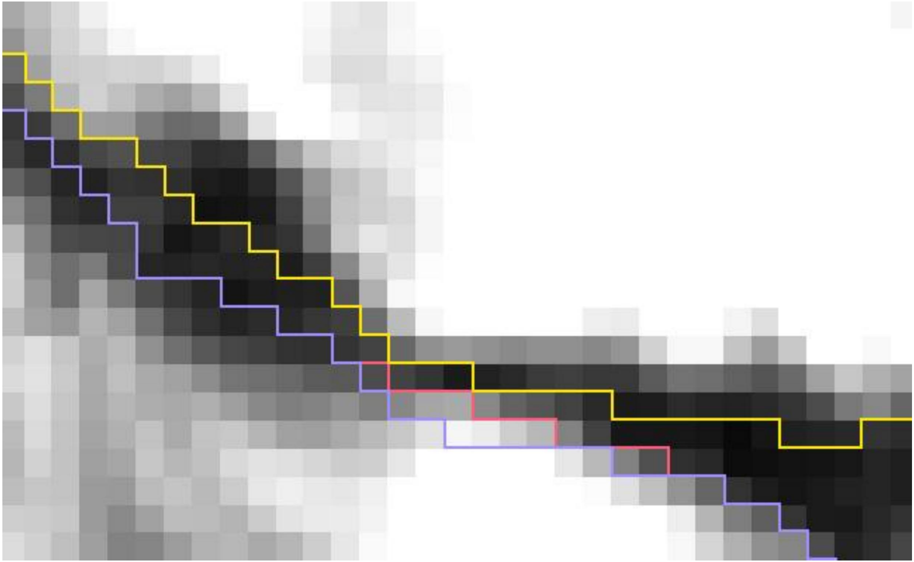

- C_0: skull (very low conductivity)
- C_1: CSF
- C_2: skin

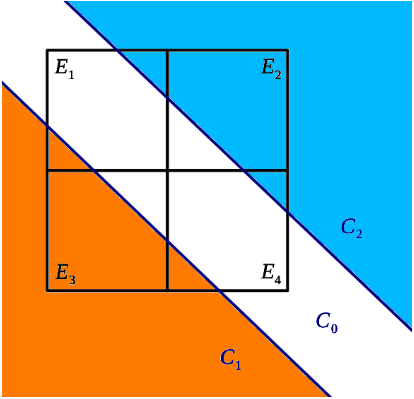

- C_0: skull (very low conductivity)
- C_1: CSF
- C_2: skin

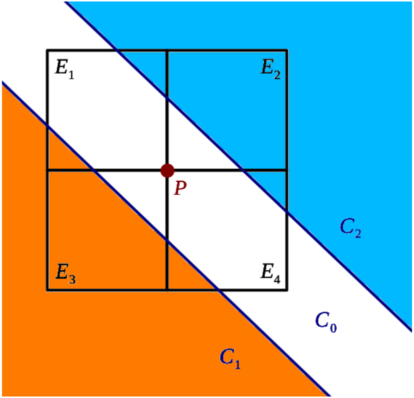

schematization: CG FEM

- C_0: skull (very low conductivity)
- C_1: CSF
- C_2: skin

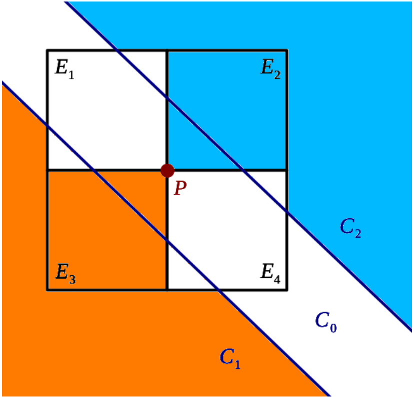

- C_0: skull (very low conductivity)
- C_1: CSF
- C_2: skin

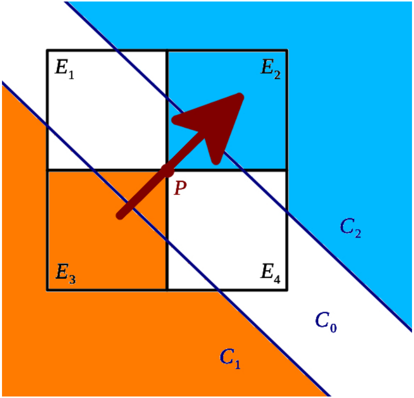

conservation of charge

$$\int_{\partial K} \sigma \nabla u \cdot \mathbf{n} ds = \int_K f_y dx$$

for any control volume $K \subset \Omega$

conservation of charge

$$\int_{\partial K} \sigma \nabla u \cdot \mathbf{n} ds = \int_K f_y dx$$

for any control volume $K \subset \Omega$

- the strong solution of the Poisson equation fulfills this property, i.e. there is a conservation property for the correction potential:

$$\int_{\partial K} \mathbf{j}^{corr} \cdot \mathbf{n} ds = \int_K f^{corr} dx$$

  where

  - $\mathbf{j}^{corr} = \sigma \nabla u^{corr}$
  - $f^{corr} = -\nabla \cdot \sigma^{corr} \nabla u^{\infty}$

conservation of charge

$$\int_{\partial K} \sigma \nabla u \cdot \mathbf{n} ds = \int_K f_y dx$$

for any control volume $K \subset \Omega$

- the strong solution of the Poisson equation fulfills this property, i.e. there is a conservation property for the correction potential:

$$\int_{\partial K} \mathbf{j}^{corr} \cdot \mathbf{n} ds = \int_K f^{corr} dx$$

  where
  - $\mathbf{j}^{corr} = \sigma \nabla u^{corr}$
  - $f^{corr} = -\nabla \cdot \sigma^{corr} \nabla u^{\infty}$
- in general, a conforming discretization does not guarantee this property

triangulation and h

A triangulation $\mathcal{T}(\Omega)$ of a domain Ω is:

- a finite set of disjoint open sets E_e
- forms a partition of Ω

h denotes the mesh width, $h := max diam(E) | E \in \mathcal{T}(\Omega)$

triangulation and h

A triangulation $\mathcal{T}(\Omega)$ of a domain Ω is:

- a finite set of disjoint open sets E_e
- forms a partition of Ω

h denotes the mesh width, $h := maxdiam(E)|E \in \mathcal{T}(\Omega)$

Broken polynomial spaces

piecewise polynomial spaces on a triangulation of Ω

$$V_h^k := \left\{ v \in L^2(\Omega) : v|_E \in \mathbb{P}^k(E) \right\},$$

where $\mathbb{P}^k$ denotes the space of polynomial functions of degree k

triangulation and h

A triangulation $\mathcal{T}(\Omega)$ of a domain Ω is:

- a finite set of disjoint open sets E_e
- forms a partition of Ω

h denotes the mesh width, $h := maxdiam(E)|E \in \mathcal{T}(\Omega)$

Broken polynomial spaces

piecewise polynomial spaces on a triangulation of Ω

$$V_h^k := \left\{ v \in L^2(\Omega) : v|_E \in \mathbb{P}^k(E) \right\},$$

where $\mathbb{P}^k$ denotes the space of polynomial functions of degree k

jump and *average* operators

$[\![u]\!] := u|_{E_e}\mathbf{n}_e + u|_{E_f}\mathbf{n}_f$, $u := \frac{\sigma_f}{\sigma_e+\sigma_f}u|_{E_e} + \frac{\sigma_e}{\sigma_e+\sigma_f}u|_{E_f}$

Symmetric Interior Penalty Galerkin (SIPG) - formulation

find $u_h^{corr} \in V_h^k$ s.t.

$$a(u_h^{corr}, v_h) + J(u_h^{corr}, v_h) = l(v_h), \forall v_h \in V_h^k$$

Symmetric Interior Penalty Galerkin (SIPG) - formulation

find $u_h^{corr} \in V_h^k$ s.t.

$$a(u_h^{corr}, v_h) + J(u_h^{corr}, v_h) = l(v_h), \forall v_h \in V_h^k$$

lhs=

$$= \int_\Omega \sigma \nabla u_h^{corr} \cdot \nabla v_h dx - \int_{\Gamma_{int}} \sigma \nabla u_h^{corr} [\![v_h]\!] ds$$
$$- \int_{\Gamma_{int}} \sigma \nabla v_h [\![u_h^{corr}]\!] ds + \eta \int_{\Gamma_{int}} \frac{\hat{\sigma}_\gamma}{h_\gamma} [\![u_h^{corr}]\!] [\![v_h]\!] ds$$

Symmetric Interior Penalty Galerkin (SIPG) - formulation

find $u_h^{corr} \in V_h^k$ s.t.

$$a(u_h^{corr}, v_h) + J(u_h^{corr}, v_h) = l(v_h), \forall v_h \in V_h^k$$

lhs=

$$= \int_\Omega \sigma \nabla u_h^{corr} \cdot \nabla v_h dx - \int_{\Gamma_{int}} \sigma \nabla u_h^{corr} [\![v_h]\!] ds$$
$$- \int_{\Gamma_{int}} \sigma \nabla v_h [\![u_h^{corr}]\!] ds + \eta \int_{\Gamma_{int}} \frac{\hat{\sigma}_\gamma}{h_\gamma} [\![u_h^{corr}]\!] [\![v_h]\!] ds$$

rhs=

$$- \int_\Omega \sigma^{corr} \nabla u^\infty \cdot \nabla v_h dx + \int_{\partial\Omega} \sigma^\infty \nabla u^\infty \cdot \mathbf{n} v ds + \int_{\Gamma_{int}} \sigma^{corr} \nabla u^\infty [\![v_h]\!] ds$$

Symmetric Interior Penalty Galerkin (SIPG) - formulation

find $u_h^{corr} \in V_h^k$ s.t.

$$a(u_h^{corr}, v_h) + J(u_h^{corr}, v_h) = l(v_h), \forall v_h \in V_h^k$$

lhs=

$$= \int_\Omega \sigma \nabla u_h^{corr} \cdot \nabla v_h dx - \int_{\Gamma_{int}} \sigma \nabla u_h^{corr} [\![v_h]\!] ds$$
$$- \int_{\Gamma_{int}} \sigma \nabla v_h [\![u_h^{corr}]\!] ds + \eta \int_{\Gamma_{int}} \frac{\hat{\sigma}_\gamma}{h_\gamma} [\![u_h^{corr}]\!] [\![v_h]\!] ds$$

rhs=

$$- \int_\Omega \sigma^{corr} \nabla u^\infty \cdot \nabla v_h dx + \int_{\partial\Omega} \sigma^\infty \nabla u^\infty \cdot \mathbf{n} v ds + \int_{\Gamma_{int}} \sigma^{corr} \nabla u^\infty [\![v_h]\!] ds$$

Symmetric Interior Penalty Galerkin (SIPG) - properties

Theorem

for $\eta > 0$ sufficiently large, the SIPG discretization has a unique solution; consistent with the strong problem

Lemma

the SIPG discretization fulfills a discrete conservation property, with

- $\vec{j}^{corr} = \{\sigma \nabla_h u_h^{corr}\} - \eta \frac{\hat{\sigma}_\gamma}{\hat{h}_\gamma} [\![u_h^{corr}]\!]$
- $f^{corr} = -\nabla \cdot \sigma^{corr} \nabla u^\infty$

schematization: DG FEM

- C_0: skull (very low conductivity)
- C_1: CSF
- C_2: skin

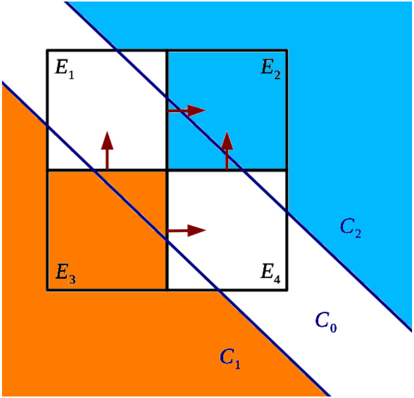

the Discontinuous Galerkin method in **EEG**

[Engwer et al., SIAM J. Scientific Comp., 2017]

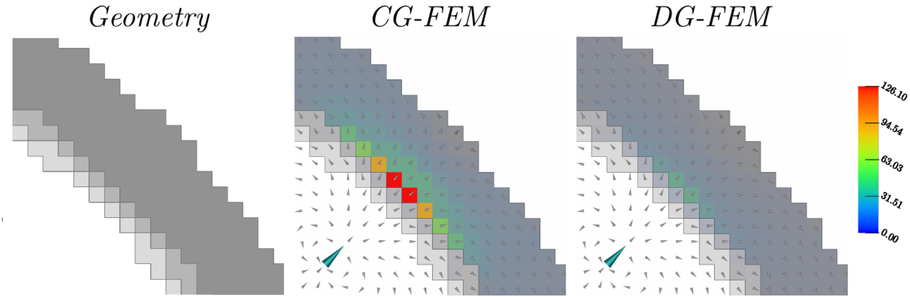

the Discontinuous Galerkin method in **EEG**

[Engwer et al., SIAM J. Scientific Comp., 2017]

the Discontinuous Galerkin method in **EEG**

[Engwer et al., SIAM J. Scientific Comp., 2017]

- fulfills the property of *conservation of charge*

the Discontinuous Galerkin method in **EEG**

[Engwer et al., SIAM J. Scientific Comp., 2017]

- fulfills the property of *conservation of charge*

a conservative flux

the electric flux $\mathbf{j}^s$ has two different representations:

$$\mathbf{j}^{s,NONcons} \text{ and } \mathbf{j}^{s,cons}$$

- $\mathbf{j}^{s,NONcons}$ does not fulfill the conservation of charge property
- $\mathbf{j}^{s,cons}$ does
- in a CG-FEM discretization only $\mathbf{j}^{s,NONcons}$ can be reppresented,
- in a DG-FEM both.

the Discontinuous Galerkin method in **EEG**

[Engwer et al., SIAM J. Scientific Comp., 2017]

- fulfills the property of *conservation of charge*

a conservative flux

the electric flux $\mathbf{j}^s$ has two different representations:

$$\mathbf{j}^{s,NONcons} \text{ and } \mathbf{j}^{s,cons}$$

- $\mathbf{j}^{s,NONcons}$ does not fulfill the conservation of charge property
- $\mathbf{j}^{s,cons}$ does
- in a CG-FEM discretization only $\mathbf{j}^{s,NONcons}$ can be reppresented,
- in a DG-FEM both.

- $\rightarrow$ curing "skull leakage" effects

the Discontinuous Galerkin method in **EEG**

[Engwer et al., SIAM J. Scientific Comp., 2017]

- fulfills the property of *conservation of charge*

a conservative flux

the electric flux $\mathbf{j}^s$ has two different representations:

$$\mathbf{j}^{s,NONcons} \text{ and } \mathbf{j}^{s,cons}$$

- $\mathbf{j}^{s,NONcons}$ does not fulfill the conservation of charge property
- $\mathbf{j}^{s,cons}$ does
- in a CG-FEM discretization only $\mathbf{j}^{s,NONcons}$ can be reppresented,
- in a DG-FEM both.

- $\rightarrow$ curing "skull leakage" effects
- uses directly voxel-based representation of the head

results

- convergence and comparison CG - DG
- leaky scenarios analysis

- 4 layer spherical head model

compartment	outer radius	conductivity
brain	78 mm	0.33 S/m
CSF	80 mm	1.79 S/m
skull	86 mm	0.01 S/m
skin	92 mm	0.49 S/m

Table: head model features

convergence and comparison

- hexahedral meshes with different resolutions (1mm, 2mm, 4mm)
- 10 randomly distributed sources for 10 different eccentricities
- relative difference measure:

$$RDM(u, v) = \left|\left| \frac{u}{||u||_2} - \frac{v}{||v||_2} \right|\right|_2$$

- logarithmic magnitude error:

$$lnMAG(u, v) = ln\left(\frac{||u||_2}{||v||_2}\right)$$

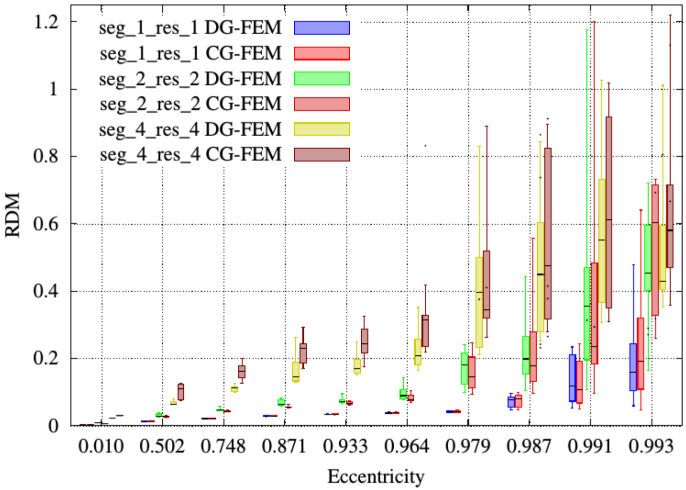

Figure: convergence - RDM

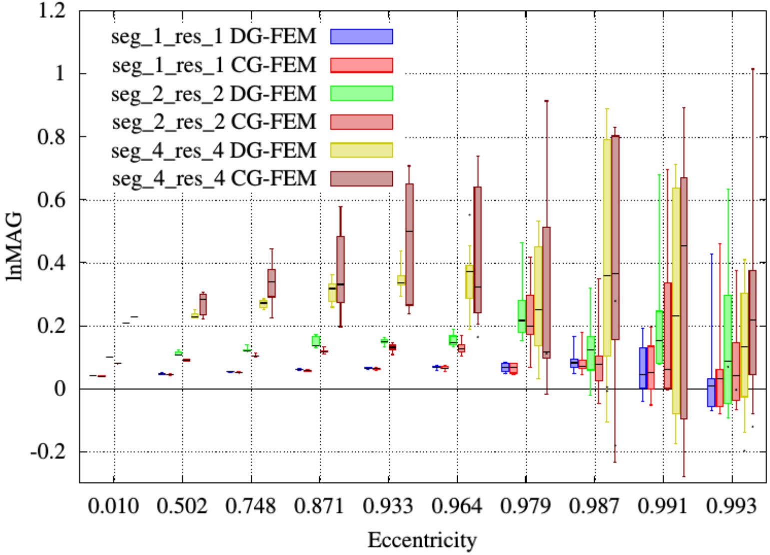

Figure: convergence - lnMAG

leaky scenario statistics

	skull thickness	num leaks
seg_2_res_2_r82	2	10,080
seg_2_res_2_r83	3	1,344
seg_2_res_2_r84	4	0

Table: leaky head models: 428,185 nodes; 407,907 elements

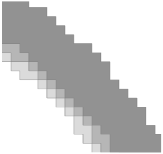

Figure: r82

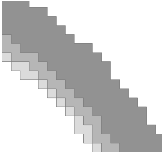

Figure: r83

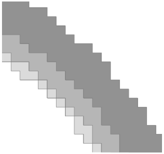

Figure: r84

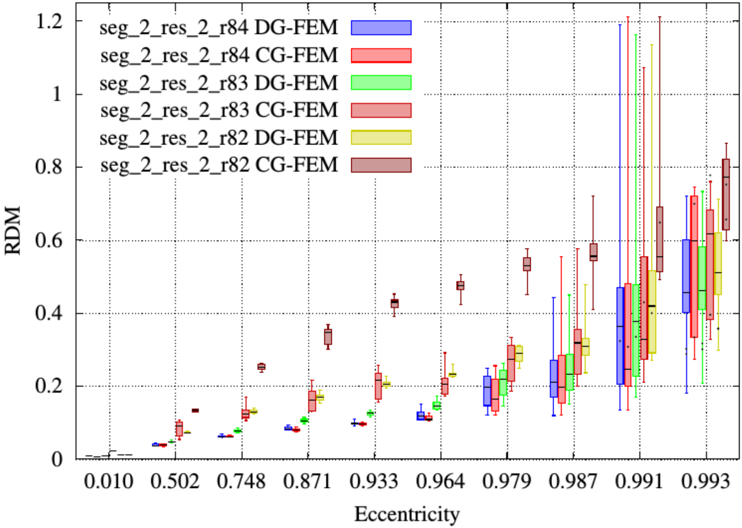

Figure: leaky - RDM

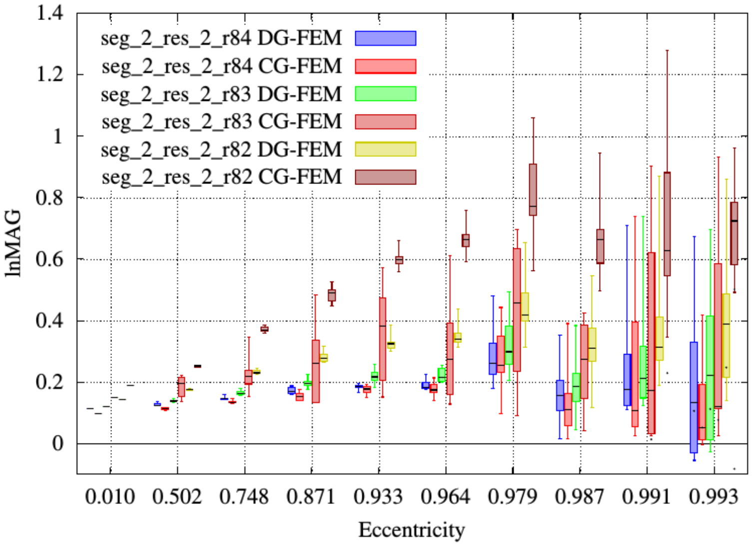

Figure: leaky - lnMAG

skull leakages of volume current - 4

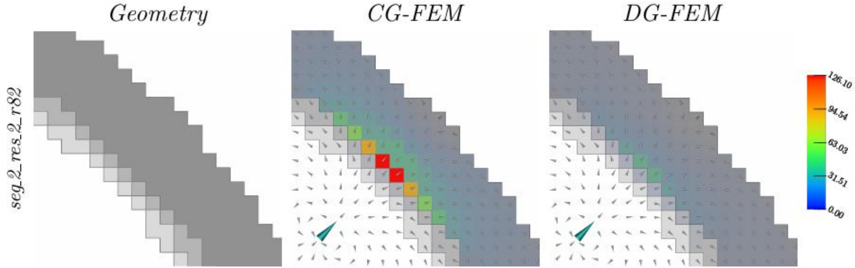

the Discontinuous Galerkin method in **MEG**

[Piastra et al., Frontiers in Neuroscience, 2018]

the Discontinuous Galerkin method in **MEG**

[Piastra et al., Frontiers in Neuroscience, 2018]

effects of fulfilling the property of *conservation of charge*?

the Discontinuous Galerkin method in **MEG**

[Piastra et al., Frontiers in Neuroscience, 2018]

effects of fulfilling the property of *conservation of charge*?
how is the general DG-FEM behavior?

the Discontinuous Galerkin method in **MEG**

[Piastra et al., Frontiers in Neuroscience, 2018]

effects of fulfilling the property of *conservation of charge*?
how is the general DG-FEM behavior?
“skull leakage” scenarios?

the Discontinuous Galerkin method in **MEG**

[Piastra et al., Frontiers in Neuroscience, 2018]

effects of fulfilling the property of *conservation of charge*?

how is the general DG-FEM behavior?

"skull leakage" scenarios?

how can this method be accessible for our Neuroscience community?

the Discontinuous Galerkin method in **MEG**

[Piastra et al., Frontiers in Neuroscience, 2018]

effects of fulfilling the property of *conservation of charge*?

how is the general DG-FEM behavior?

"skull leakage" scenarios?

how can this method be accessible for our Neuroscience community?

the Discontinuous Galerkin method in **MEG**

[Piastra et al., Frontiers in Neuroscience, 2018]

effects of fulfilling the property of *conservation of charge*?

how is the general DG-FEM behavior?

"skull leakage" scenarios?

how can this method be accessible for our Neuroscience community?

$$\mathbf{B}^s(\mathbf{r}) = \frac{\mu_0}{4\pi} \int_\Omega \mathbf{j}^s(\mathbf{r}') \times \frac{\mathbf{r} - \mathbf{r}'}{|\mathbf{r} - \mathbf{r}'|^3} \, d^3\mathbf{r}'$$

the Discontinuous Galerkin method in **MEG**

[Piastra et al., Frontiers in Neuroscience, 2018]

effects of fulfilling the property of *conservation of charge*?

how is the general DG-FEM behavior?

"skull leakage" scenarios?

how can this method be accessible for our Neuroscience community?

$$\mathbf{B}^s(\mathbf{r}) = \frac{\mu_0}{4\pi} \int_\Omega \mathbf{j}^s(\mathbf{r}') \times \frac{\mathbf{r} - \mathbf{r}'}{|\mathbf{r} - \mathbf{r}'|^3} \, d^3\mathbf{r}'$$

- $\mathbf{B}^{s,NONcons}(\mathbf{r}) = \frac{\mu_0}{4\pi} \int_\Omega \mathbf{j}^{s,NONcons}(\mathbf{r}') \times \frac{\mathbf{r}-\mathbf{r}'}{|\mathbf{r}-\mathbf{r}'|^3} \, d^3\mathbf{r}'$

the Discontinuous Galerkin method in **MEG**

[Piastra et al., Frontiers in Neuroscience, 2018]

effects of fulfilling the property of *conservation of charge*?

how is the general DG-FEM behavior?

"skull leakage" scenarios?

how can this method be accessible for our Neuroscience community?

$$\mathbf{B}^s(\mathbf{r}) = \frac{\mu_0}{4\pi} \int_\Omega \mathbf{j}^s(\mathbf{r}') \times \frac{\mathbf{r}-\mathbf{r}'}{|\mathbf{r}-\mathbf{r}'|^3}\, d^3\mathbf{r}'$$

- $\mathbf{B}^{s,NONcons}(\mathbf{r}) = \frac{\mu_0}{4\pi} \int_\Omega \mathbf{j}^{s,NONcons}(\mathbf{r}') \times \frac{\mathbf{r}-\mathbf{r}'}{|\mathbf{r}-\mathbf{r}'|^3}\, d^3\mathbf{r}'$
- $\mathbf{B}^{s,cons}(\mathbf{r}) = \frac{\mu_0}{4\pi} \int_\Omega \mathbf{j}^{s,cons}(\mathbf{r}') \times \frac{\mathbf{r}-\mathbf{r}'}{|\mathbf{r}-\mathbf{r}'|^3}\, d^3\mathbf{r}'$

the Discontinuous Galerkin method in **MEG**

[Piastra et al., Frontiers in Neuroscience, 2018]

effects of fulfilling the property of *conservation of charge*?

how is the general DG-FEM behavior?

“skull leakage” scenarios?

how can this method be accessible for our Neuroscience community?

simulation in a sphere model

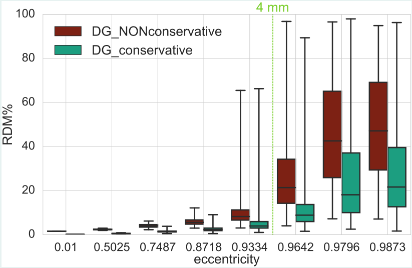

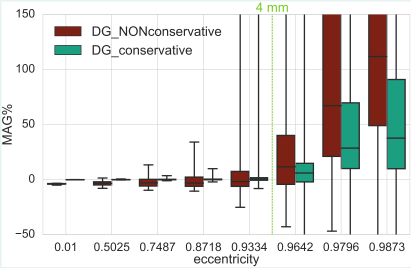

the Discontinuous Galerkin method in **MEG**

[Piastra et al., Frontiers in Neuroscience, 2018]

effects of fulfilling the property of *conservation of charge*?

how is the general DG-FEM behavior?

"skull leakage" scenarios?

how can this method be accessible for our Neuroscience community?

the Discontinuous Galerkin method in **MEG**

[Piastra et al., Frontiers in Neuroscience, 2018]

effects of fulfilling the property of *conservation of charge*?

how is the general DG-FEM behavior?

"skull leakage" scenarios?

how can this method be accessible for our Neuroscience community?

sphere model

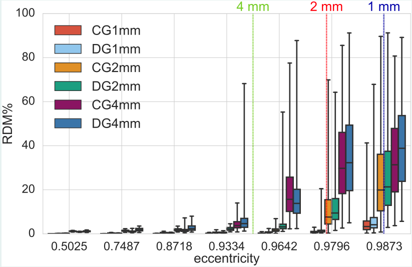

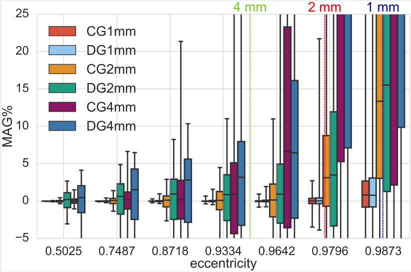

the Discontinuous Galerkin method in **MEG**

[Piastra et al., Frontiers in Neuroscience, 2018]

effects of fulfilling the property of *conservation of charge*?

how is the general DG-FEM behavior?

“skull leakage” scenarios?

how can this method be accessible for our Neuroscience community?

sphere model: RDM% mean= 1.5% and MAG% mean = 0.1%

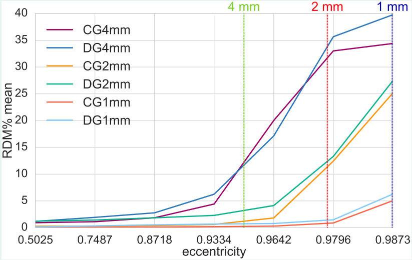

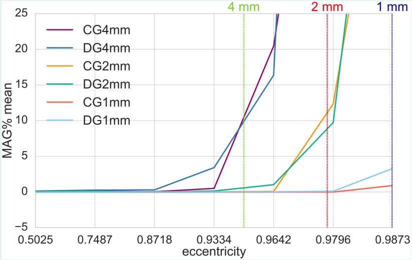

the Discontinuous Galerkin method in **MEG**

[Piastra et al., Frontiers in Neuroscience, 2018]

effects of fulfilling the property of *conservation of charge*?

how is the general DG-FEM behavior?

“skull leakage” scenarios?

how can this method be accessible for our Neuroscience community?

the Discontinuous Galerkin method in **MEG**

[Piastra et al., Frontiers in Neuroscience, 2018]

effects of fulfilling the property of *conservation of charge*?

how is the general DG-FEM behavior?

"skull leakage" scenarios?

how can this method be accessible for our Neuroscience community?

simulation in a sphere model with leakages

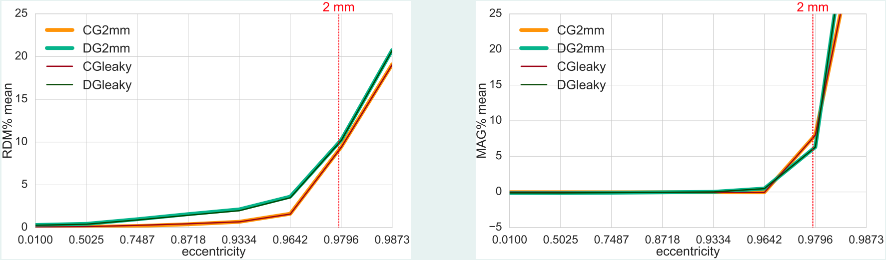

the Discontinuous Galerkin method in **MEG**

[Piastra et al., Frontiers in Neuroscience, 2018]

effects of fulfilling the property of *conservation of charge*?

how is the general DG-FEM behavior?

"skull leakage" scenarios?

how can this method be accessible for our Neuroscience community?

the Discontinuous Galerkin method in **MEG**

[Piastra et al., Frontiers in Neuroscience, 2018]

effects of fulfilling the property of *conservation of charge*?
how is the general DG-FEM behavior?
"skull leakage" scenarios?
how can this method be accessible for our Neuroscience community?

simulation tool

the Discontinuous Galerkin method in **MEG**

[Piastra et al., Frontiers in Neuroscience, 2018]

effects of fulfilling the property of *conservation of charge*?

how is the general DG-FEM behavior?

"skull leakage" scenarios?

how can this method be accessible for our Neuroscience community?

simulation tool

- C++ open source library for solving **partial differential equations (PDEs)**

Dune http://dune-project.org/

the Discontinuous Galerkin method in **MEG**

[Piastra et al., Frontiers in Neuroscience, 2018]

effects of fulfilling the property of *conservation of charge*?
how is the general DG-FEM behavior?
"skull leakage" scenarios?
how can this method be accessible for our Neuroscience community?

simulation tool

- C++ open source library for solving **partial differential equations (PDEs)**
- solving PDEs in **Neuroscience**

Dune
http://dune-project.org/

duneuro
http://duneuro.org/

the Discontinuous Galerkin method in **MEG**

[Piastra et al., Frontiers in Neuroscience, 2018]

effects of fulfilling the property of *conservation of charge*?
how is the general DG-FEM behavior?
"skull leakage" scenarios?
how can this method be accessible for our Neuroscience community?

simulation tool

- C++ open source library for solving **partial differential equations (PDEs)**
  Dune
  http://dune-project.org/
- solving PDEs in **Neuroscience**
  duneuro
  http://duneuro.org/
- integration of **duneuro** in **FieldTrip**
  FieldTrip

summary

the Discontinuous Galerkin method in **MEG**

[Piastra et al., Frontiers in Neuroscience, 2018]

summary

- a conservative representation of the flux increases the accuracy of DG-FEM results in MEG

the Discontinuous Galerkin method in **MEG**

[Piastra et al., Frontiers in Neuroscience, 2018]

summary

- a conservative representation of the flux increases the accuracy of DG-FEM results in MEG
- for the finest mesh resolution of 1 mm, sources with a distance of 1.59 mm from the brain-CSF surface, DG-FEM yielded mean RDM% of 1.5% and mean MAG% of 0.1% for the magnetic field

the Discontinuous Galerkin method in **MEG**

[Piastra et al., Frontiers in Neuroscience, 2018]

summary

- a conservative representation of the flux increases the accuracy of DG-FEM results in MEG
- for the finest mesh resolution of 1 mm, sources with a distance of 1.59 mm from the brain-CSF surface, DG-FEM yielded mean RDM% of 1.5% and mean MAG% of 0.1% for the magnetic field
- skull leakages do not play a role for the MEG modality

the Discontinuous Galerkin method in **MEG**

[Piastra et al., Frontiers in Neuroscience, 2018]

summary

- a conservative representation of the flux increases the accuracy of DG-FEM results in MEG
- for the finest mesh resolution of 1 mm, sources with a distance of 1.59 mm from the brain-CSF surface, DG-FEM yielded mean RDM% of 1.5% and mean MAG% of 0.1% for the magnetic field
- skull leakages do not play a role for the MEG modality
- in a combined EEG and MEG (EMEG) source reconstruction analysis is desirable to employ the same forward model for both EEG and MEG data

the Discontinuous Galerkin method in **MEG**

[Piastra et al., Frontiers in Neuroscience, 2018]

summary

- a conservative representation of the flux increases the accuracy of DG-FEM results in MEG
- for the finest mesh resolution of 1 mm, sources with a distance of 1.59 mm from the brain-CSF surface, DG-FEM yielded mean RDM% of 1.5% and mean MAG% of 0.1% for the magnetic field
- skull leakages do not play a role for the MEG modality
- in a combined EEG and MEG (EMEG) source reconstruction analysis is desirable to employ the same forward model for both EEG and MEG data
- DG-FEM complements, and in some cases as the skull leakage scenarios, outperforms CG-FEM in EEG or combined EMEG

the Discontinuous Galerkin method in **MEG**

[Piastra et al., Frontiers in Neuroscience, 2018;12:30]

proof of concept:

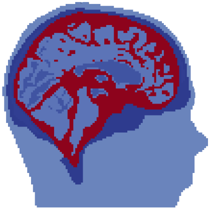

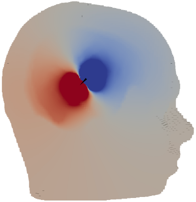

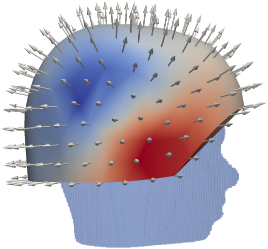

outline

- general introduction
- continuous Galerkin for EEG and MEG
- discontinuous Galerkin for EEG and MEG
- unfitted discontinuous Galerkin for EEG
- summary

the Unfitted Discontinuous Galerkin method in **EEG**

[Nüßing et al., IEEE Trans. on Biom. Eng., 2016]

- good conservative properties of the DG-FEM

the Unfitted Discontinuous Galerkin method in **EEG**

[Nüßing et al., IEEE Trans. on Biom. Eng., 2016]

- good conservative properties of the DG-FEM
- uses hexahedral meshes

the Unfitted Discontinuous Galerkin method in **EEG**

[Nüßing et al., IEEE Trans. on Biom. Eng., 2016]

- good conservative properties of the DG-FEM
- uses hexahedral meshes
- eliminates geometrical error

the Unfitted Discontinuous Galerkin method in **EEG**

[Nüßing et al., IEEE Trans. on Biom. Eng., 2016]

- good conservative properties of the DG-FEM
- uses hexahedral meshes
- eliminates geometrical error
- obtains same accuracy as DG-FEM in tetrahedral model

the Unfitted Discontinuous Galerkin method in **EEG**

[Nüßing et al., IEEE Trans. on Biom. Eng., 2016]

- good conservative properties of the DG-FEM
- uses hexahedral meshes
- eliminates geometrical error
- obtains same accuracy as DG-FEM in tetrahedral model
- ouperforms DG-FEM in hexahedral model

the Unfitted Discontinuous Galerkin method in **EEG**

[Nüßing et al., IEEE Trans. on Biom. Eng., 2016]

- good conservative properties of the DG-FEM
- uses hexahedral meshes
- eliminates geometrical error
- obtains same accuracy as DG-FEM in tetrahedral model
- ouperforms DG-FEM in hexahedral model
- controlled computational costs

the Unfitted Discontinuous Galerkin method in **EEG**

[Nüßing et al., IEEE Trans. on Biom. Eng., 2016]

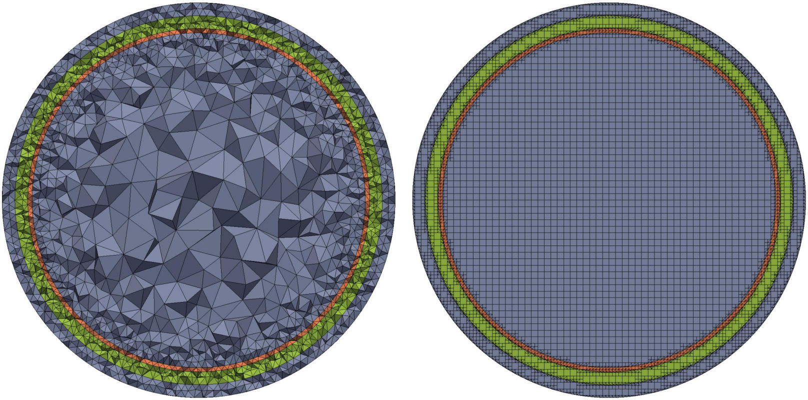

the Unfitted Discontinuous Galerkin method in **EEG**

[Nüßing et al., IEEE Trans. on Biom. Eng., 2016]

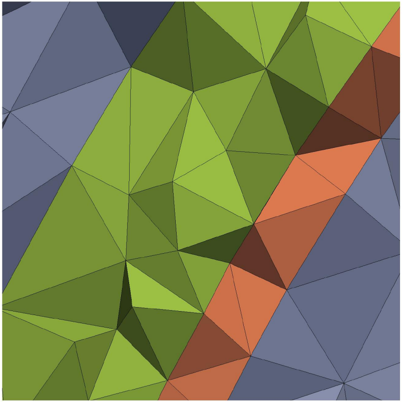

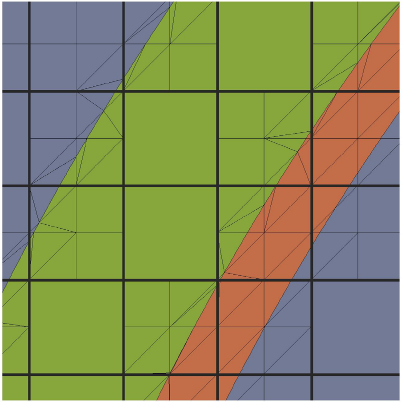

outline

- general introduction
- continuous Galerkin for EEG and MEG
- discontinuous Galerkin for EEG and MEG
- unfitted discontinuous Galerkin for EEG
- summary

summary

- the subtraction approach cures the singularity on the right-hand side of the EEG forward problem (Wolters et al., 2007; Drechsler et al., 2009)

summary

- the subtraction approach cures the singularity on the right-hand side of the EEG forward problem (Wolters et al., 2007; Drechsler et al., 2009)
- CG-FEM can suffer from skull leakages (directly in EEG (Engwer et al., 2017), indirectly in MEG (Piastra et al., 2018))

summary

- the subtraction approach cures the singularity on the right-hand side of the EEG forward problem (Wolters et al., 2007; Drechsler et al., 2009)
- CG-FEM can suffer from skull leakages (directly in EEG (Engwer et al., 2017), indirectly in MEG (Piastra et al., 2018))
- SIPG (DG) - FEM fulfills conservation law, it has the same accuracy as CG-FEM and voxel-based representations can be used directly (Engwer et al., 2017)

- the subtraction approach cures the singularity on the right-hand side of the EEG forward problem (Wolters et al., 2007; Drechsler et al., 2009)
- CG-FEM can suffer from skull leakages (directly in EEG (Engwer et al., 2017), indirectly in MEG (Piastra et al., 2018))
- SIPG (DG) - FEM fulfills conservation law, it has the same accuracy as CG-FEM and voxel-based representations can be used directly (Engwer et al., 2017)
- UDG-FEM use level set function directly and outperforms DG-FEM on hexahedral meshes (Nüßing et al., 2016)

Structure

- Validation of different FEM forward approaches in TES and EEG
- CutFEM
- Mixed FEM

[Vogenauer, Master Thesis in Mathematics, 2019]
[Piastra,…, Wolters, *Frontiers in Neurosci., 2018*]
[Engwer, Vorwerk, Ludewig & Wolters, *SIAM J. Sci. Comp., 2017*]

Validation and evaluation of new FEM forward approaches

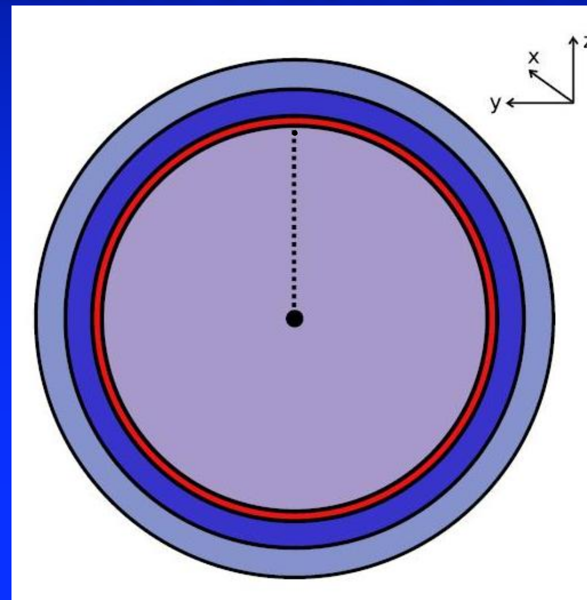

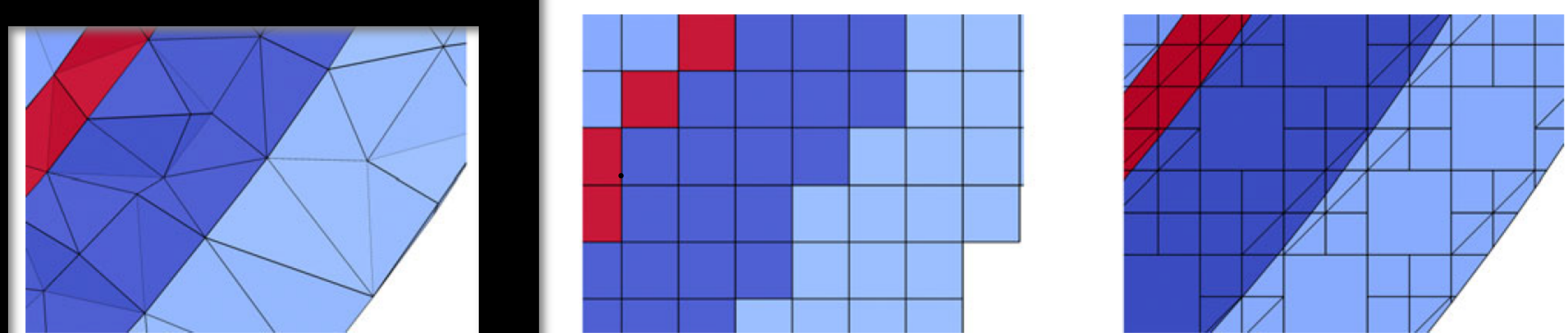

(a) (b) (c)

[redacted] multilayer sphere verification. From left to right, the images show the *DG-tet-1447k*, *DG-hex-3057k*, and [redacted] different conductivity values. (a) Conforming tetrahedral mesh. (b) Conforming hexahedral mesh. (c) Cut cell mesh.

TES: Validation and evaluation of surface-based tetrahedral FEM

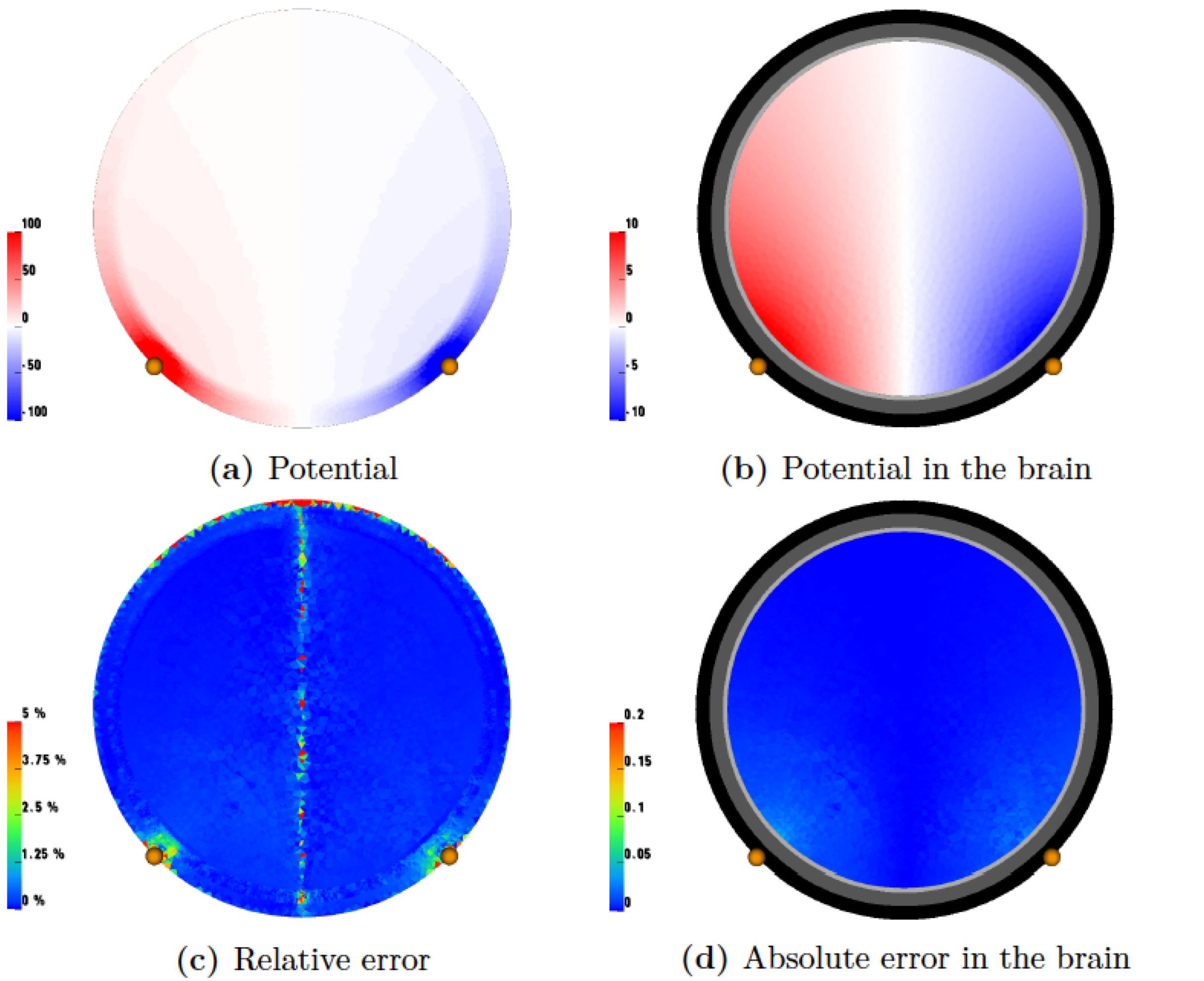

Figure 5.3.: The numerical solution in the tet-4layer-434k sphere model for tES forward problem **(a)** in the whole volume conductor and **(b)** just the brain compartment. Visualization of the **(c)** relative error and **(d)** the absolute error between numerical and analytical solution in the brain compartment.

[Vogenauer, Master Thesis in Mathematics, 2019]
[Piastra,…, Wolters, *Frontiers in Neurosci., 2018*]
[Engwer, Vorwerk, Ludewig & Wolters, *SIAM J. Sci. Comp., 2017*]

Validation and evaluation of new FEM forward approaches

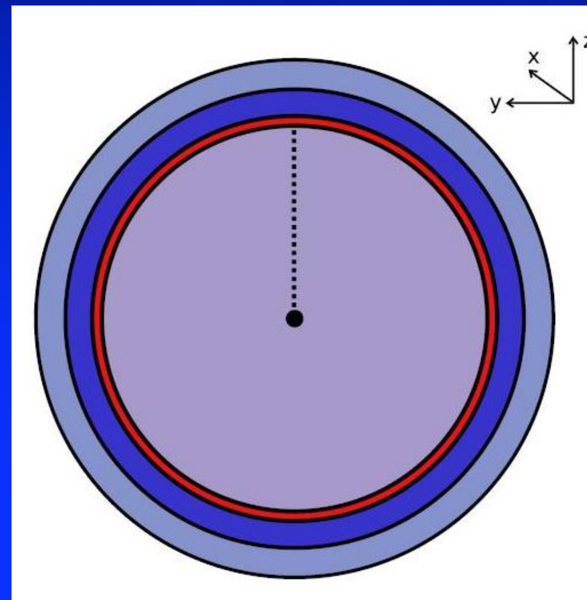

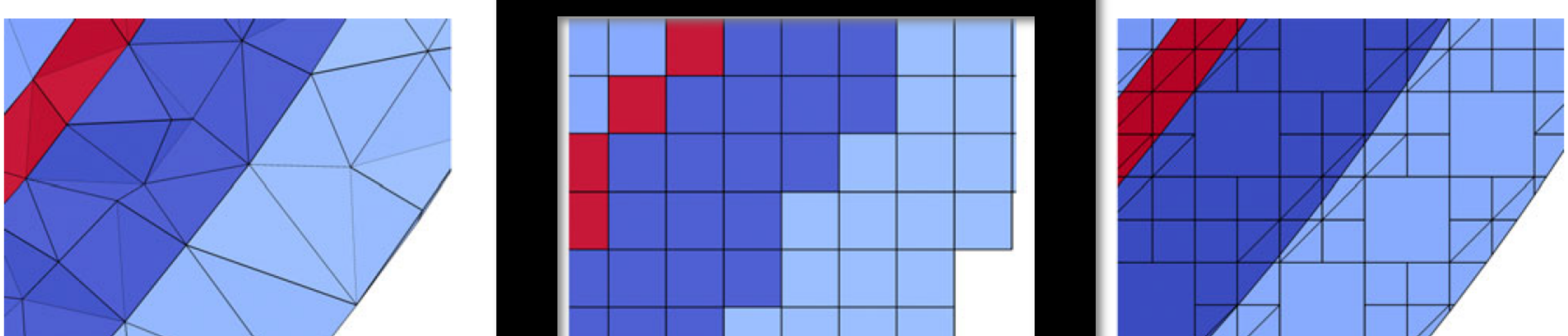

(a) (b) (c)

Fig. 3. Sections of the different meshes used in th[redacted]ages show the *DG-tet-1447k*, *DG-hex-3057k*, and *UDG-1335k* models. The different colors represent the different conductivity values. (a) Conforming tetrahedral mesh. (b) Conforming hexahedral mesh. (c) Cut cell mesh.

[Vogenauer, Master Thesis in Mathematics, 2019]
[Piastra,…, Wolters, *Frontiers in Neurosci., 2018*]
[Engwer, Vorwerk, Ludewig & Wolters, *SIAM J. Sci. Comp., 2017*]

TES: Validation of Continuous Galerkin (CG) and Discontinuous Galerkin (DG) FEM in 2 mm hexahedral meshes with 4 mm skull thickness

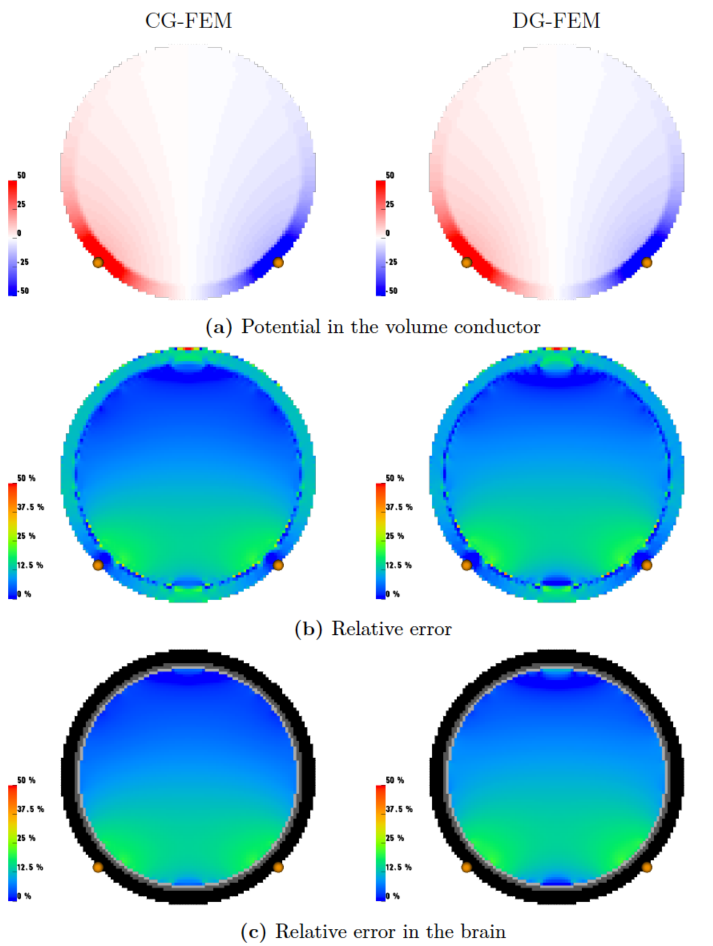

Figure 5.9.: Numerical results for hex-res-2mm-r84 sphere model CG-FEM (left) and DG-FEM (right). First, the potential solution is shown **(a)** in the sphere model. Then visualizations of the relative error **(b)** in the whole volume conductor and **(c)** only in the brain compartment are shown.

[Vogenauer, Master Thesis in Mathematics, 2019]
[Piastra,…, Wolters, *Frontiers in Neurosci., 2018*]
[Engwer, Vorwerk, Ludewig & Wolters, *SIAM J. Sci. Comp., 2017*]

TES: Validation of Continuous Galerkin (CG) and Discontinuous Galerkin (DG) FEM in 2 mm hexahedral meshes with 2 mm skull thickness

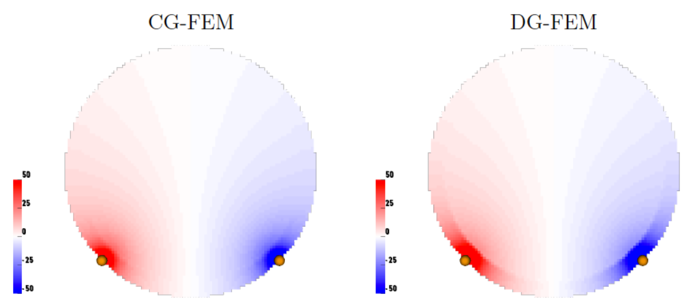

(a) Potential in the volume conductor

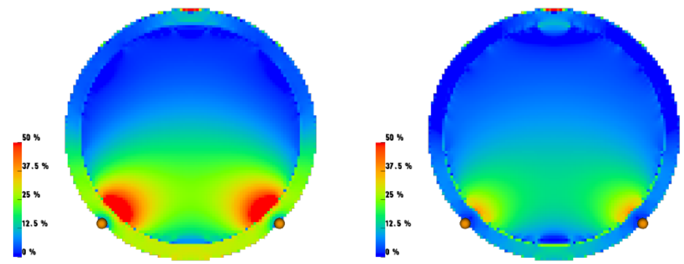

(b) Relative error

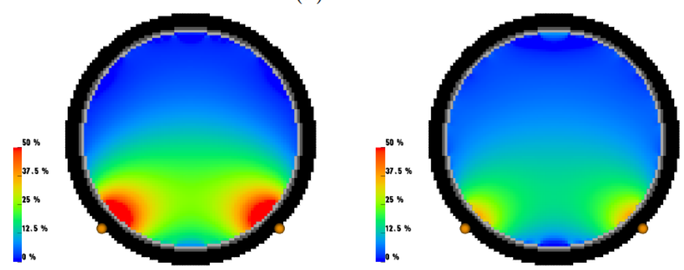

(c) Relative error in the brain

Figure 5.11.: Numerical results for hex-res-2mm-r82 sphere model CG-FEM (left) and DG-FEM (right). First, the potential solution is shown **(a)** in the sphere model. Then visualizations of the relative error **(b)** in the whole volume conductor and **(c)** only in the brain compartment are shown.

[Vogenauer, Master Thesis in Mathematics, 2019]
[Piastra,…, Wolters, *Frontiers in Neurosci., 2018*]
[Engwer, Vorwerk, Ludewig & Wolters, *SIAM J. Sci. Comp., 2017*]

”Skull leakages” when using standard FEM in insufficiently resolved hexahedral models

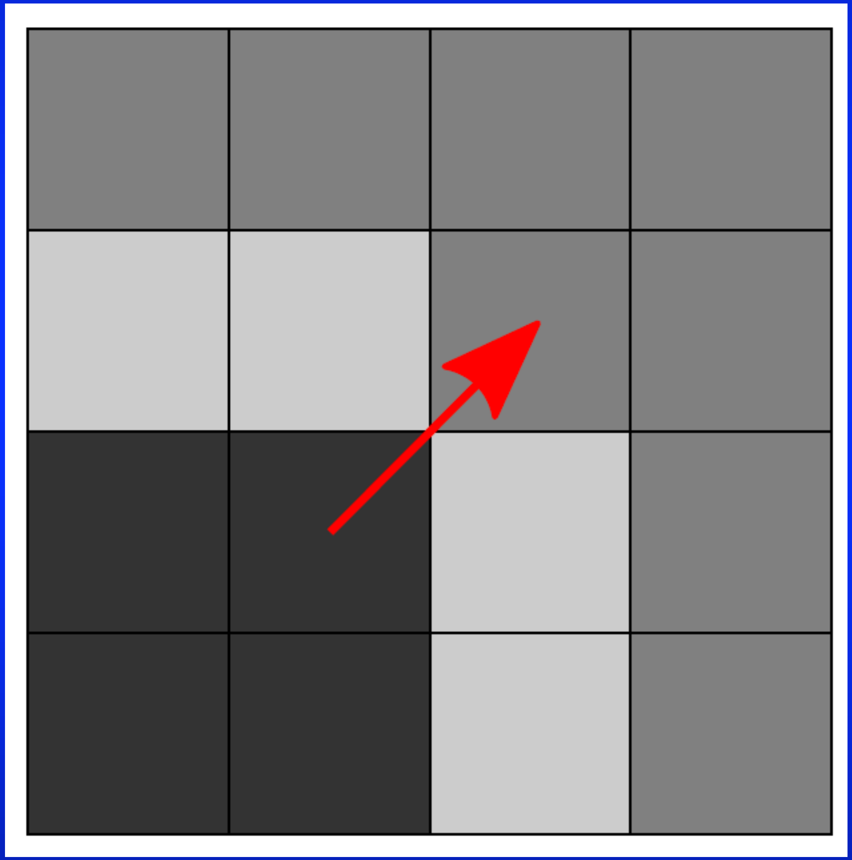

CG-FEM: Unphysical current flow through an FE node

Discontinuous Galerkin- (DG-) FEM in hexahedral models

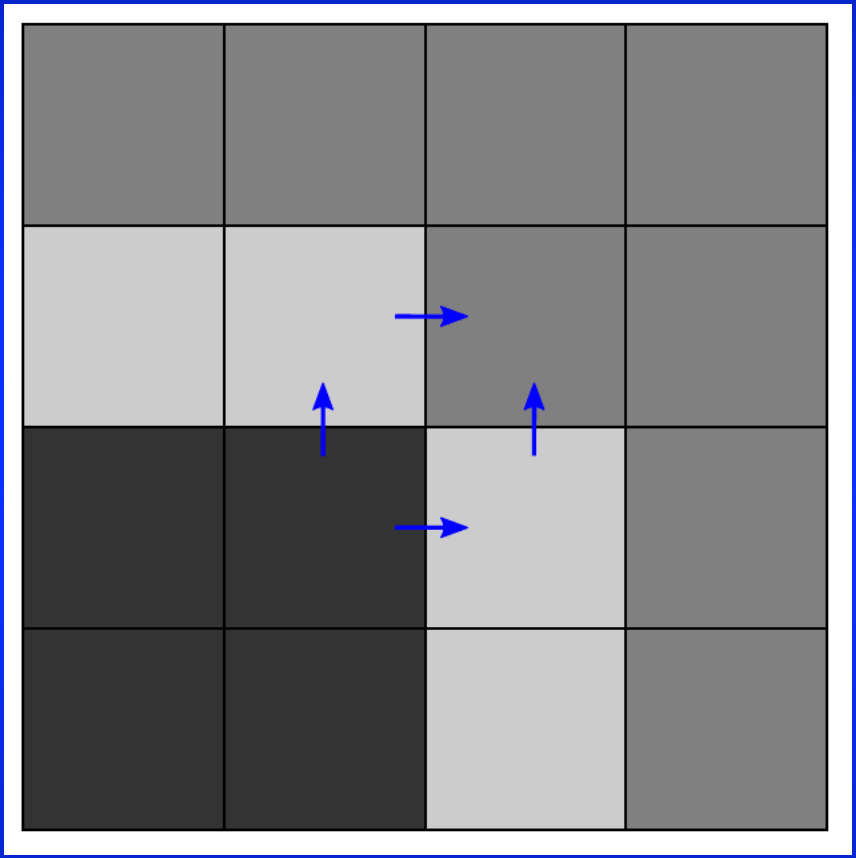

DG-FEM:
Continuous radial current flow component over tissue boundaries
Discontinuous potential over tissue boundaries

[Vogenauer, Master Thesis in Mathematics, 2019]
[Piastra,…, Wolters, *Frontiers in Neurosci., 2018*]
[Engwer, Vorwerk, Ludewig & Wolters, *SIAM J. Sci. Comp., 2017*]

Validation and evaluation of new FEM forward approaches

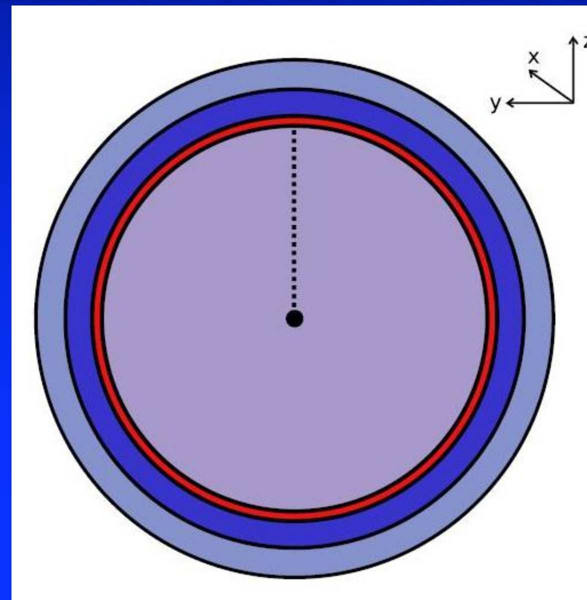

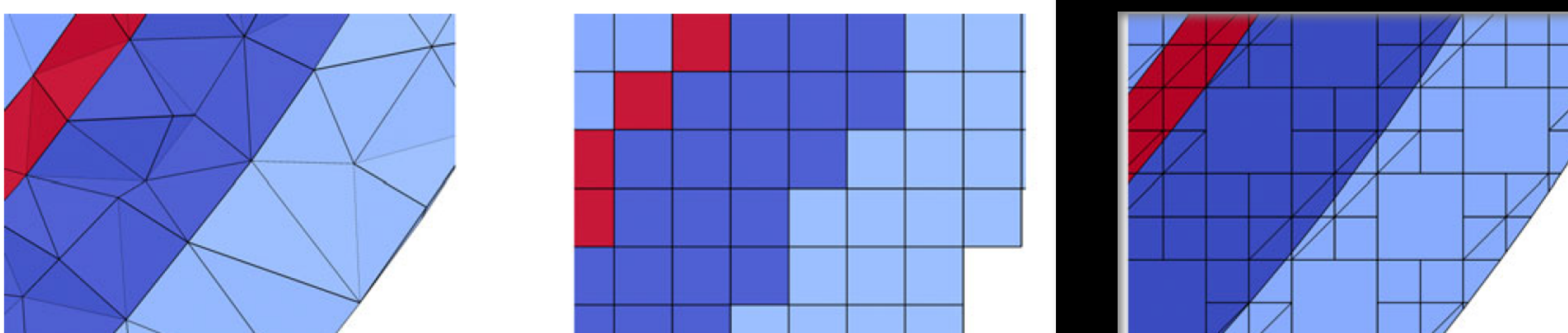

(a) (b) (c)

Fig. 3. Sections of the different meshes used in the multilayer sphere verification. From left to right, t[redacted] *UDG-1335k* models. The different colors represent the different conductivity values. (a) Conforming tetrahedral mesh. (b) Conforming hexahedral mesh. (c) Cut cell mesh.

[Nüßing, Wolters, Brinck & Engwer,…UDG-FEM for EEG..., *IEEE Trans Biomed Eng, 2016*]

EEG: Validation of Unfitted DG (UDG) FEM

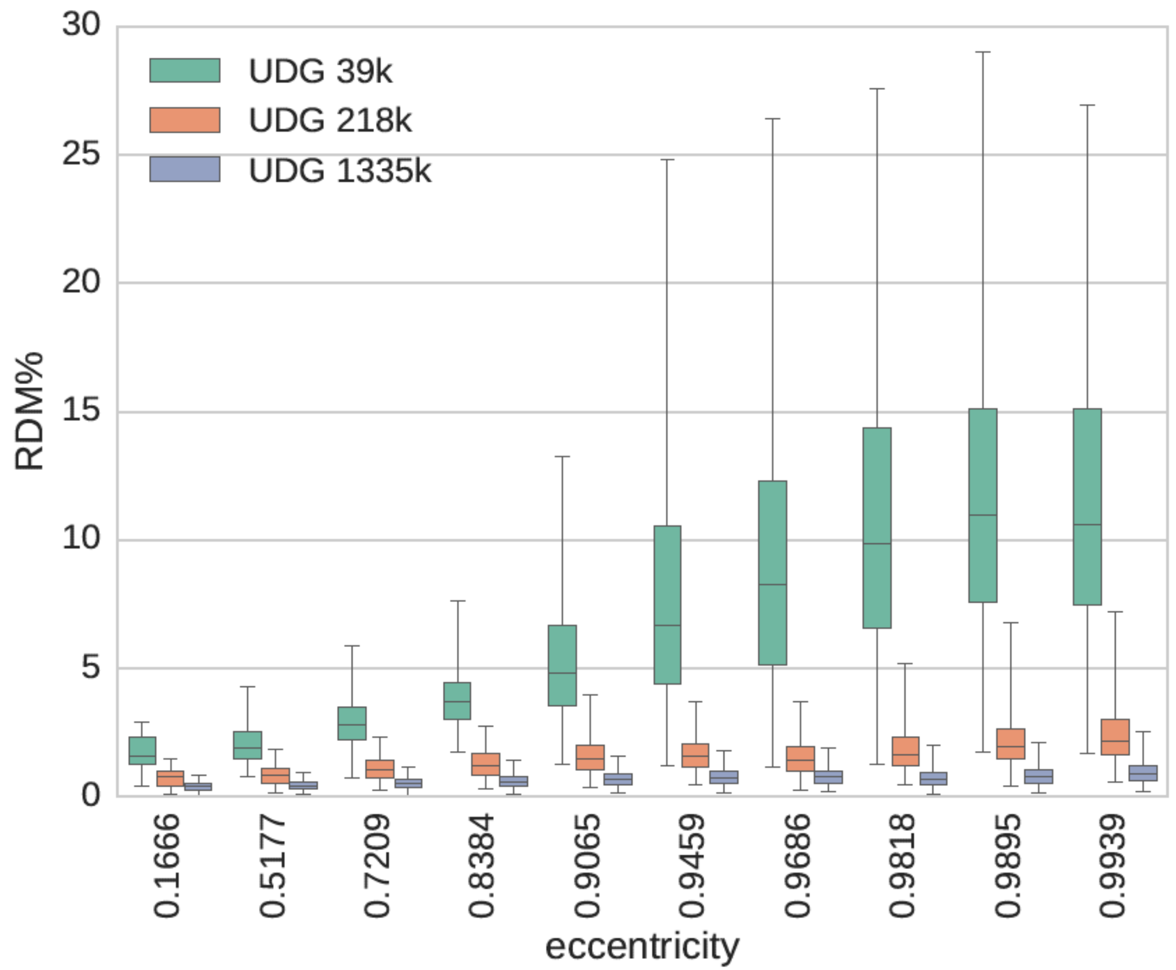

(a) RDM% error for radial dipoles

[Nüßing, Wolters, Brinck & Engwer,…UDG-FEM for EEG..., *IEEE Trans Biomed Eng, 2016*]

EEG: Validation of Unfitted DG (UDG) FEM

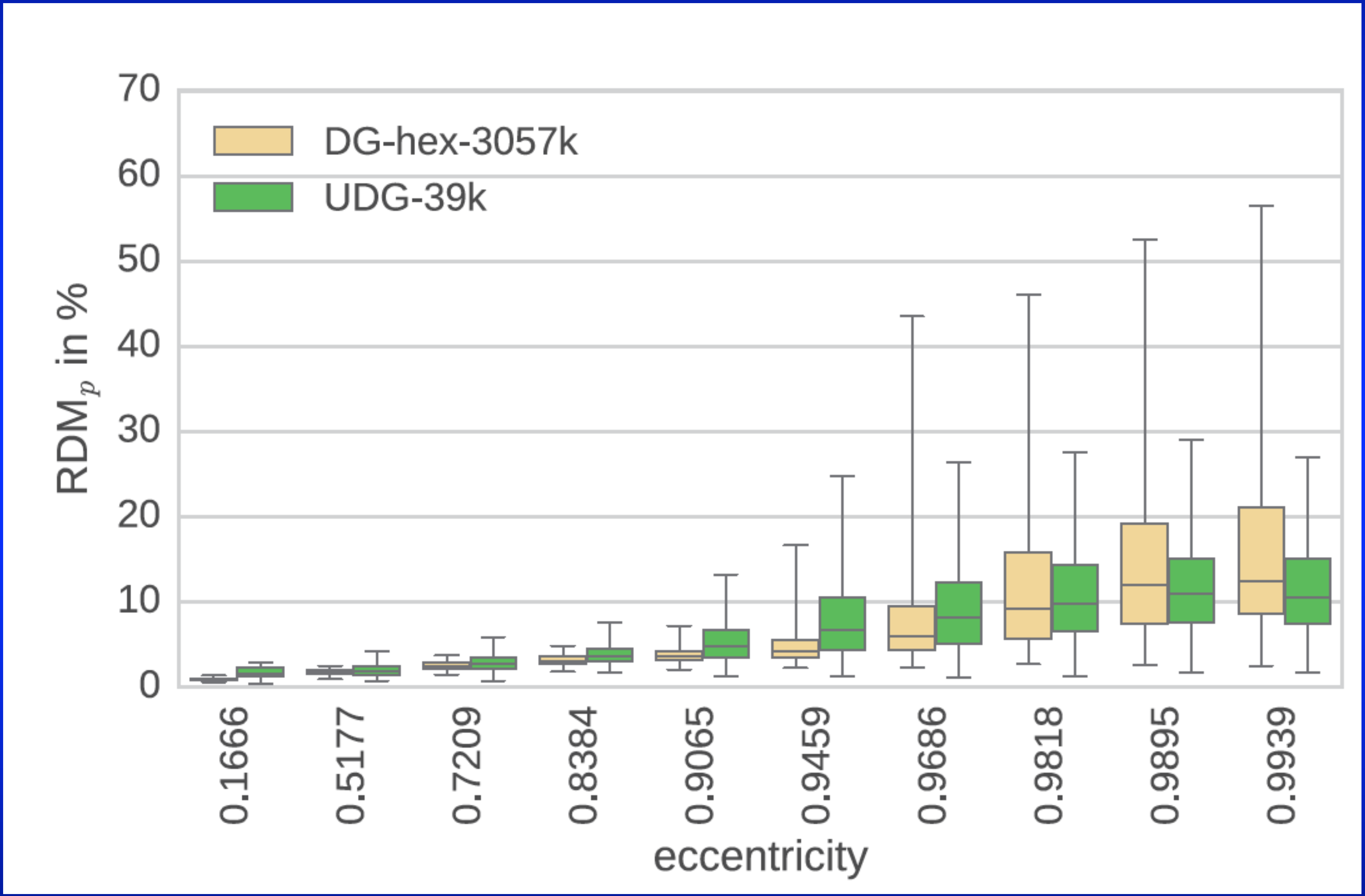

Structure

- Validation of different FEM forward approaches in TES and EEG
- CutFEM
- Mixed FEM

[Erdbrügger, *Master thesis in Maths, 2021*]
[Nüßing, *PhD thesis in Maths, 2018*]

Level sets and cut elements

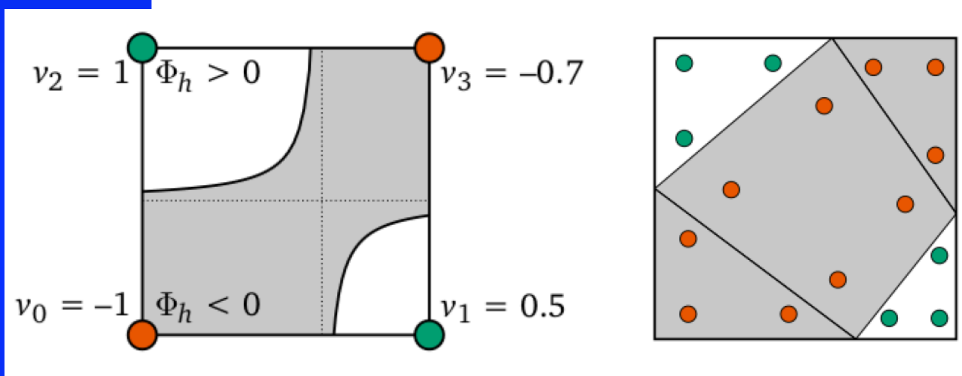

a) Reconstruction of one cut element([Nüß18])

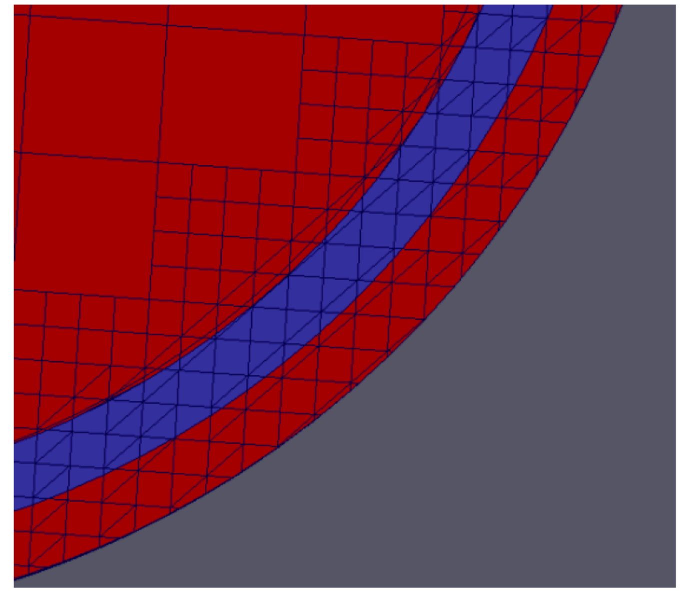

b) Reconstruction of a multilayer sphere model.

Fig. 4.7.: a) Reconstruction of a single square cut by a level-set. The grey area indicates the inside of the domain, reconstructed into 5 cut-cells, 3 of which are inside the domain. The red points indicate quadrature points for the domain, the green are for the outside area. b) Reconstruction of a multilayer sphere model. Accurate depiction of the curvature of the sphere is achieved while maintaining a low fundamental mesh resolution.

[Erdbrügger, *Master thesis in Maths, 2021*]
[Nüßing, *PhD thesis in Maths, 2018*]

CutFEM for tDCS and EEG

Definition 4.4 (weak tDCS-/EEG CutFEM formulation) *Find $u_h \in V_h$ such that*

$$a(u_h, v_h) + a^N_{n/s}(u_h, v_h) + a^G(u_h, v_h) = l(v_h)\ \forall v_h \in V_h \tag{4.23}$$

with

- $l(v_h) = \int_{\partial\Omega} I v_h dS$ *for tDCS and*
- $l(v_h) = -\sum_i \int_{\Omega_i} \nabla J^p v_h^i dx$ *for EEG.*

$$a(u_h, v_h) = \sum_i \int_{\Omega_i} \sigma \nabla u_h^i \nabla v_h^i dx$$

In total, the Nitsche coupling terms with Symmetric Weighted Interior Penalty Galerkin (SWIPG) are stated as

$$a_s^N(u_h, v_h) := -\int_\Gamma \{\sigma \nabla u_h\}[\![v_h]\!] - \int_\Gamma \{\sigma \nabla v_h\}[\![u_h]\!] dS + \gamma \nu_k \int_\Gamma \frac{\hat{\sigma}}{\hat{h}} [\![u_h]\!][\![v_h]\!] dS, \tag{4.18}$$

or in the Non-Symmetric (NWIPG) case as

$$a_n^N(u_h, v_h) := -\int_\Gamma \{\sigma \nabla u_h\}[\![v_h]\!] + \int_\Gamma \{\sigma \nabla v_h\}[\![u_h]\!] dS + \gamma \nu_k \int_\Gamma \frac{\hat{\sigma}}{\hat{h}} [\![u_h]\!][\![v_h]\!] dS, \tag{4.19}$$

the two only differing in one sign.

Then the Ghost-penalty term can be stated as

$$a^G(u_h, v_h) = \gamma_G \int_{\hat{\Gamma}} \hat{h} [\![\sigma \nabla u_h]\!][\![\nabla v_h]\!] dS.$$

Comparing CutFEM and CG-FEM

[Erdbrügger, *Master thesis in Maths, 2021*]
[Nüßing, *PhD thesis in Maths, 2018*]

In total, CutFEM features several differences compared to standard CG-FEM.

- Using the level-set function directly allows for a very accurate representation of the head geometry.
- No possibly complicated mesh generation as in the tetrahedral case is necessary. Misshapen cut-cells are taken care of through Ghost-penalties.
- Ansatzfunctions are defined on the fundamental mesh. This can be chosen coarser than a CG-mesh while maintaining a similar level of accuracy. Thus the number of Degrees of Freedom (i.e. number of Ansatzfunctions) is smaller.
- Most mesh-generators cannot deal with holes in the compartments, which occur for example in the CSF when brain and skull touch.
- A possible downside is the dependence on the penalty parameters γ, γ_G which can strongly influence the result as will be seen in the evaluations.

[Erdbrügger, *Master thesis in Maths, 2021*]

Comparing CutFEM and CG-FEM

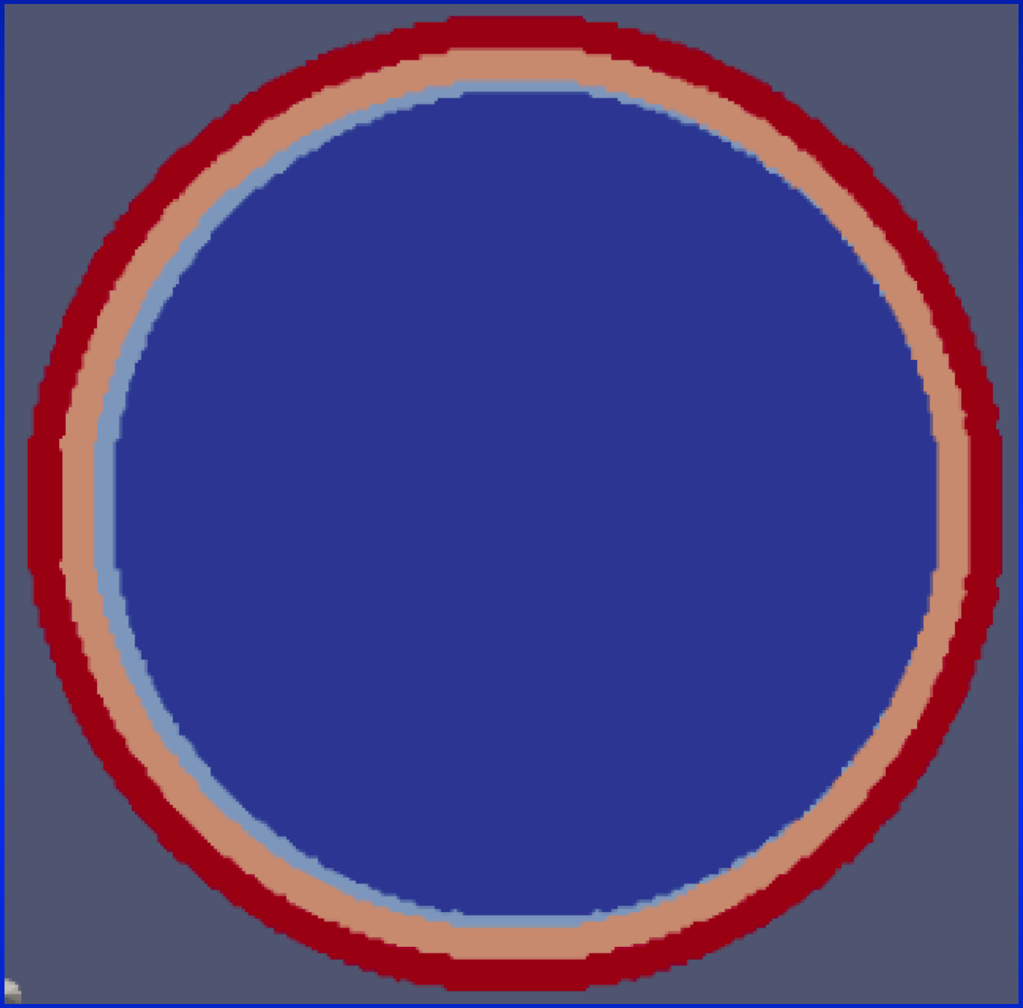

Fig. 6.1.: Depiction of the 4-layer-sphere model used. The layers from red to blue are scalp, skull, CSF and brain. The brain is shifted to the right, thus shares exactly one point with the skull.

[Erdbrügger, *Master thesis in Maths, 2021*]

Comparing CutFEM and CG-FEM for EEG

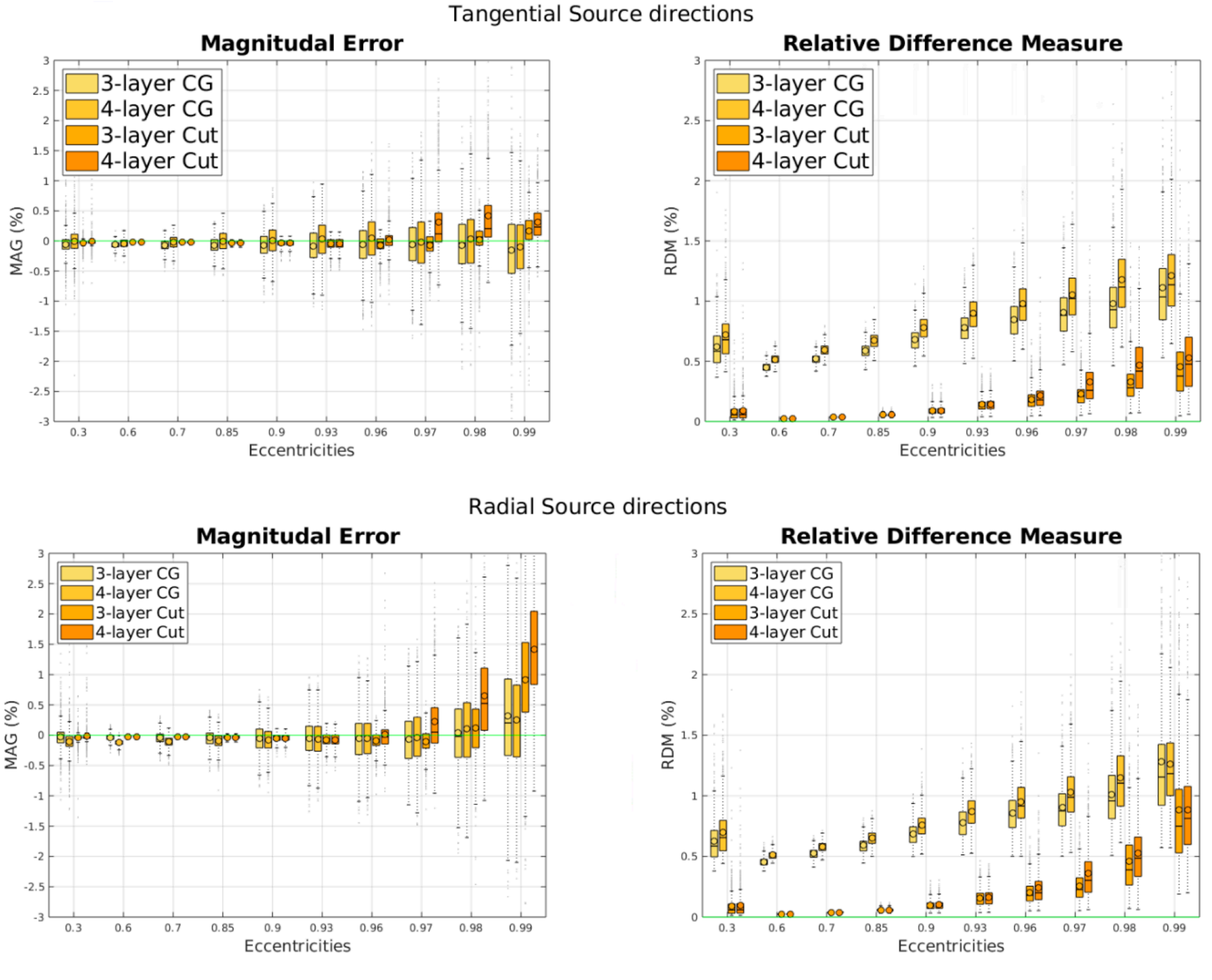

Fig. 6.14.: Overview of different EEG-errors for 3- and 4-layer CG- and CutFEM. Top: Errors for tangential source directions. Bottom: Errors for radial source directions. Errors are in percent and grouped by eccentricities. The green line marks optimal error values, the circle represents the average error.

NWIPG approach with Nitsche-penalty 40 and Ghost-penalty 0.05

Comparing CutFEM and CG-FEM for TES

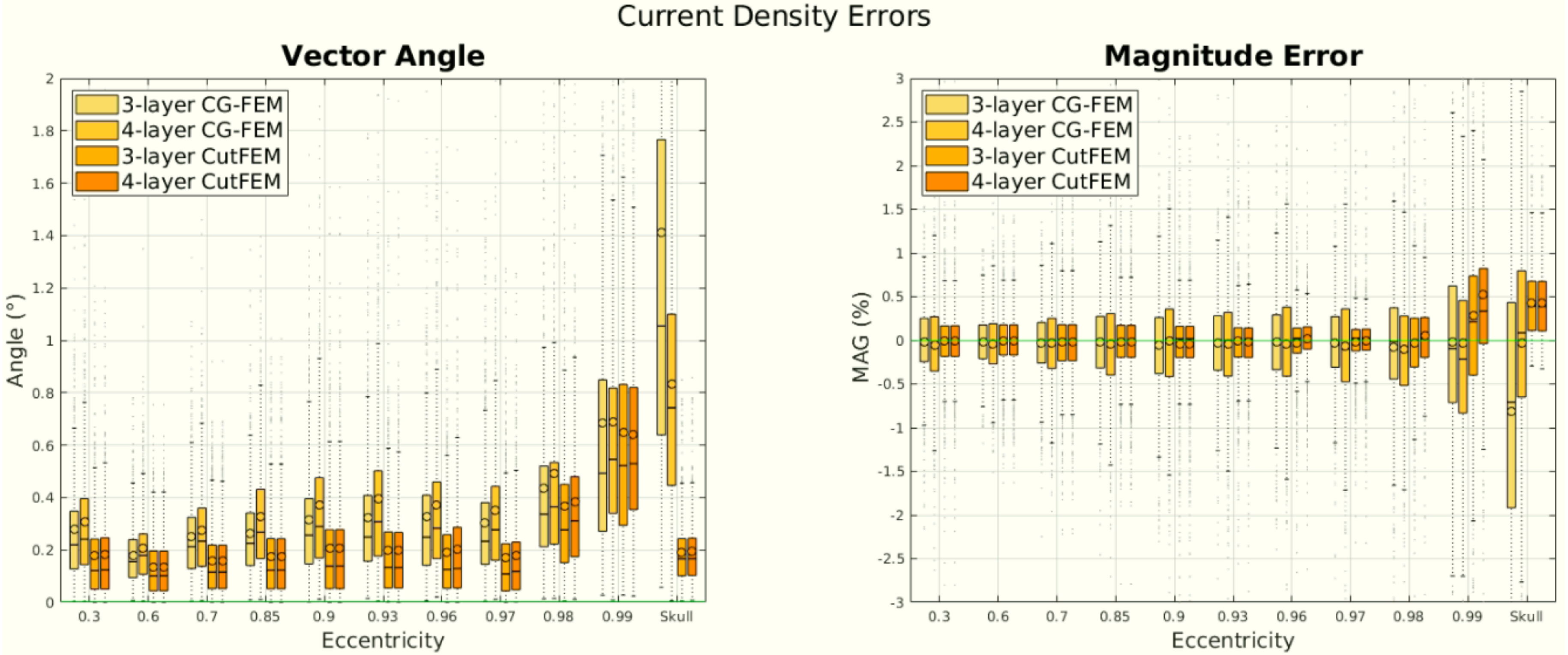

Fig. 6.15.: Overview of different tDCS-errors for 3- and 4-layer CG- and CutFEM. Right: Vector Magnitude differences in percent. The green lines indicate optimal values, the circle depicts the average error per category.

NWIPG approach with Nitsche-penalty 40 and Ghost-penalty 0.05

Comparing CutFEM and CG-FEM for TES

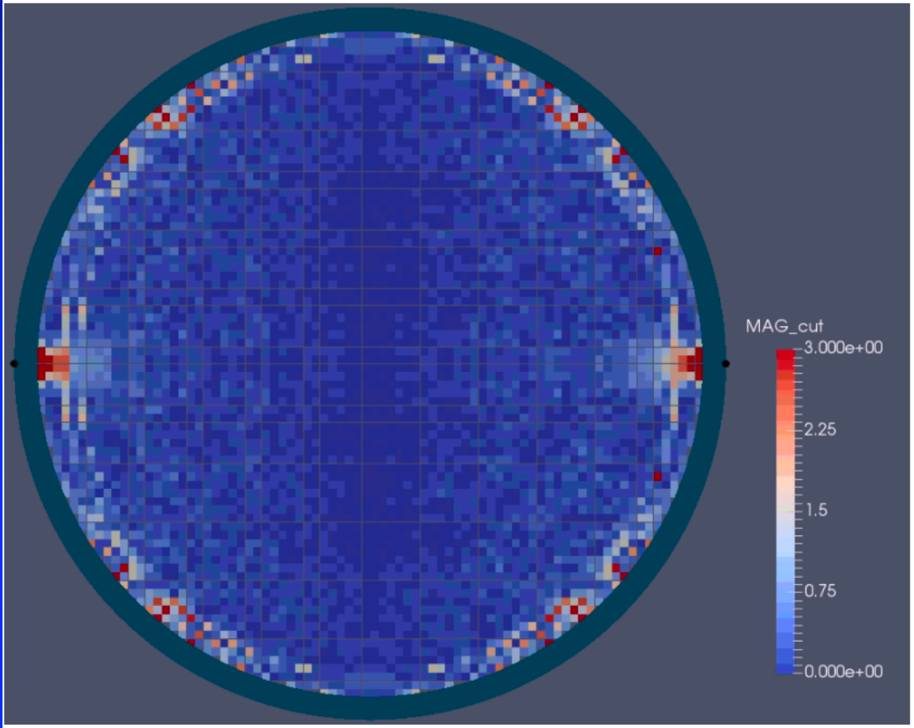

a) CutFEM

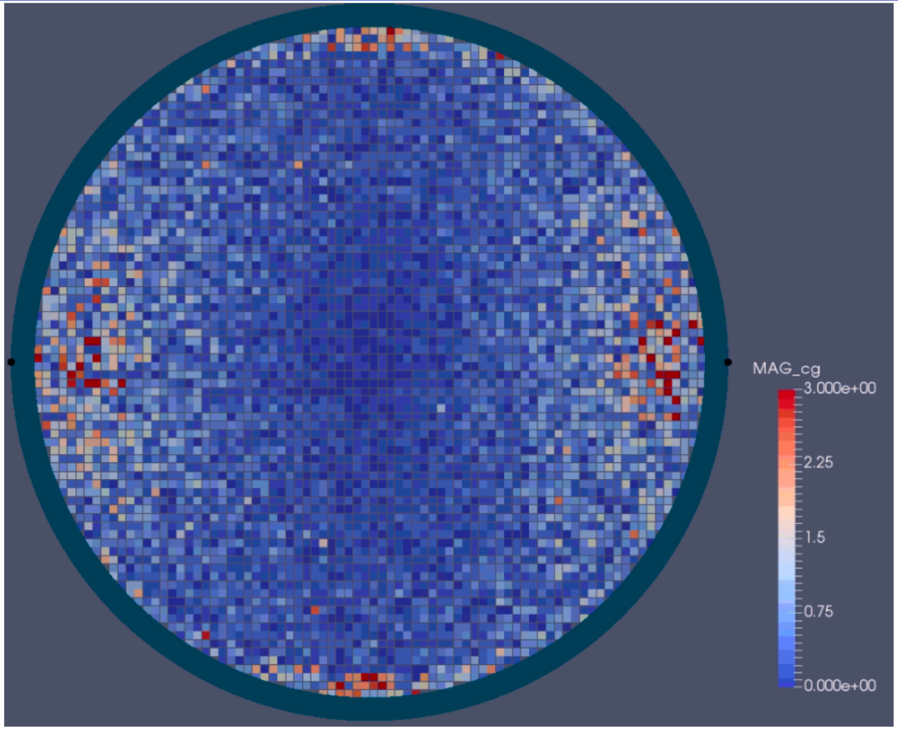

b) CG-FEM

Fig. 6.18.: Comparison of absolute MAG errors for Cut- and CGFEM. Left: CutFEM. Right: CG-FEM. Fundamental mesh cells are colorised by MAG at the center. For a clearer comparison, the CG-errors stem from the nearest tetrahedral center, the MAG error at that point was then used to colorize the fundamental cell. Brightest color is reached at 3 percent. Scalp cells are ignored to improve clarity. Instead, the entire scalp area is depicted as single color sphere. Black dots indicate stimulation electrodes.

NWIPG approach with Nitsche-penalty 40 and Ghost-penalty 0.05

[Erdbrügger, *Master thesis in Maths, 2021*]

Comparing CutFEM and CG-FEM for TES

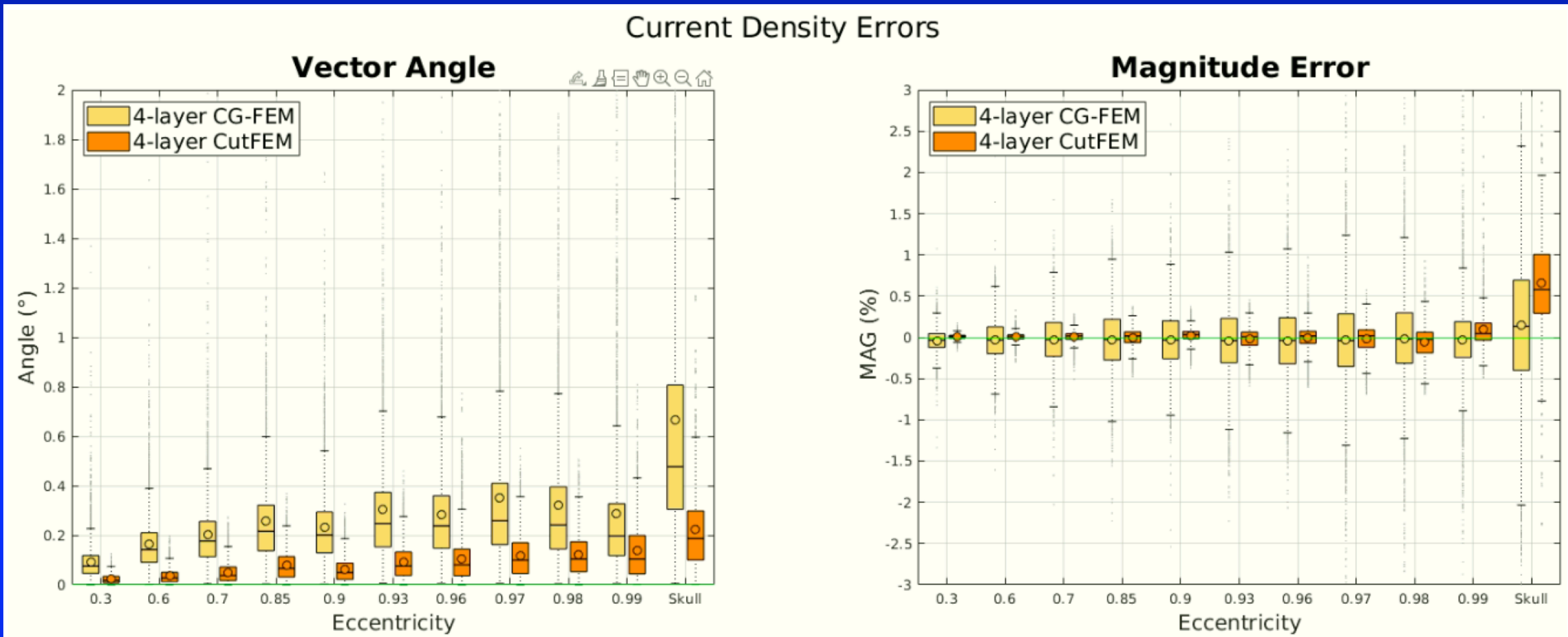

Fig. 6.19.: Overview of different tDCS-errors for 3- and 4-layer CG- and CutFEM taken at element centers. Right: Vector Magnitude differences in percent. The green lines indicate optimal values, the circle depicts the average error per category.

NWIPG approach with Nitsche-penalty 40 and Ghost-penalty 0.05

Structure

- Validation of different FEM forward approaches in TES and EEG
- CutFEM
- Mixed FEM

[Vorwerk, Engwer, Pursiainen & Wolters, *IEEE Trans Med Imag, 2017*]

Mixed FEM

Applying the quasistatic approximation of Maxwell's equations [18], [19], the forward problem of EEG is commonly formulated as a second-order PDE with homogeneous Neumann boundary condition

$$\nabla \cdot (\sigma \nabla u) = \nabla \cdot \mathbf{j}^p \quad \text{in } \Omega, \tag{1a}$$

$$\sigma \partial_{\mathbf{n}} u = 0 \quad \text{on } \partial\Omega = \Gamma. \tag{1b}$$

Here, u denotes the electric potential, $\mathbf{j}^p$ the source current, and σ the conductivity distribution in Ω. In (1), the electric current $\mathbf{j}$ is already eliminated as an unknown. For our purpose, we start at the previous step in the derivation of the quasistatic approximation and keep the electric current as an unknown.

Thus, our starting point is the system of first-order PDEs

$$\mathbf{j} + \sigma \nabla u = \mathbf{j}^p \tag{2a}$$

$$\nabla \cdot \mathbf{j} = 0 \quad \text{in } \Omega, \tag{2b}$$

$$\langle \mathbf{j}, \mathbf{n} \rangle = \langle \mathbf{j}^p, \mathbf{n} \rangle \quad \text{on } \partial\Omega = \Gamma. \tag{2c}$$

Since the source current $\mathbf{j}^p$ in general fulfills $\langle \mathbf{j}^p, \mathbf{n} \rangle = 0$ on Γ, as supp $\mathbf{j}^p \subset \Omega^\circ$ for physiological reasons (there are no sources in the skin), (2c) can be simplified to $\langle \mathbf{j}, \mathbf{n} \rangle = 0$ on Γ. The Mixed-FEM formulation for the EEG forward problem is now derived from (2), instead of discretizing (1) as would be done for the CG-FEM.

[Vorwerk, Engwer, Pursiainen & Wolters, *IEEE Trans Med Imag, 2017*]

Mixed FEM

$$\mathbf{j} + \sigma \nabla u = \mathbf{j}^p \tag{2a}$$

$$\nabla \cdot \mathbf{j} = 0 \quad \text{in } \Omega, \tag{2b}$$

$$\langle \mathbf{j}, \mathbf{n} \rangle = \langle \mathbf{j}^p, \mathbf{n} \rangle \quad \text{on } \partial\Omega = \Gamma. \tag{2c}$$

$$H(\mathrm{div}; \Omega) = \left\{ \mathbf{q} \in L^2(\Omega)^3 : \nabla \cdot \mathbf{q} \in L^2(\Omega) \right\}$$

$$H_0(\mathrm{div}, \Omega) = \{ \mathbf{q} \in H(\mathrm{div}; \Omega) : \langle \mathbf{q}, \mathbf{n} \rangle = 0 \text{ on } \partial\Omega \}$$

Now, we can introduce a weak formulation of (2)

$$\int_\Omega \langle \sigma^{-1} \mathbf{j}, \mathbf{q} \rangle \, \mathrm{d}x - \int_\Omega \nabla \cdot \mathbf{q} u \, \mathrm{d}x = \int_\Omega \langle \sigma^{-1} \mathbf{j}^p, \mathbf{q} \rangle \, \mathrm{d}x \quad \text{for all } \mathbf{q} \in H_0(\mathrm{div}, \Omega), \tag{6a}$$

$$\int_\Omega \nabla \cdot \mathbf{j} v \, \mathrm{d}x = 0 \quad \text{for all } v \in L^2(\Omega). \tag{6b}$$

Mixed FEM

Now, we can introduce a weak formulation of (2)

$$\int_\Omega \langle \sigma^{-1}\mathbf{j}, \mathbf{q}\rangle \, \mathrm{d}x - \int_\Omega \nabla \cdot \mathbf{q} u \, \mathrm{d}x = \int_\Omega \langle \sigma^{-1}\mathbf{j}^p, \mathbf{q}\rangle \, \mathrm{d}x \quad \text{for all } \mathbf{q} \in H_0(\mathrm{div}, \Omega), \tag{6a}$$

$$\int_\Omega \nabla \cdot \mathbf{j} v \, \mathrm{d}x = 0 \quad \text{for all } v \in L^2(\Omega). \tag{6b}$$

$$a(\mathbf{p}, \mathbf{q}) = (\sigma^{-1}\mathbf{p}, \mathbf{q})_{L^2(\Omega)^3}, \tag{7a}$$

$$b(\mathbf{p}, v) = (\nabla \cdot \mathbf{p}, v)_{L^2(\Omega)} \tag{7b}$$

and the functional

$$l(\mathbf{q}) = (\sigma^{-1}\mathbf{j}^p, \mathbf{q})_{L^2(\Omega)^3} \tag{7c}$$

for $\mathbf{p}, \mathbf{q} \in H_0(\mathrm{div}, \Omega)$, $v \in L^2(\Omega)$, $\mathbf{j}^p \in L^2(\Omega)^3$, $\sigma \in L^\infty(\Omega)$, $\sigma > 0$. Therefore, to solve (6) is to

find $(u, \mathbf{j}) \in L^2(\Omega) \times H_0(\mathrm{div}, \Omega)$, such that

$$a(\mathbf{j}, \mathbf{q}) + b(\mathbf{q}, u) = l(\mathbf{q}) \quad \text{for all } \mathbf{q} \in H_0(\mathrm{div}, \Omega), \tag{8a}$$

$$b(\mathbf{j}, v) = 0 \quad \text{for all } v \in L^2(\Omega). \tag{8b}$$

Mixed FEM

find $(u, \mathbf{j}) \in L^2(\Omega) \times H_0(\mathrm{div}, \Omega)$, such that

$$a(\mathbf{j}, \mathbf{q}) + b(\mathbf{q}, u) = l(\mathbf{q}) \quad \text{for all } \mathbf{q} \in H_0(\mathrm{div}, \Omega), \tag{8a}$$

$$b(\mathbf{j}, v) = 0 \quad \text{for all } v \in L^2(\Omega). \tag{8b}$$

We can now choose the space P_0 of piecewise constant functions on each element as a discrete subspace of $L^2(\Omega)$:

$$P_0(\mathcal{T}_h) = \left\{ v \in L^2(\Omega) : v|_T \equiv c_T,\ c_T \in \mathbb{R} \text{ for all } T \in \mathcal{T}_h \right\}.$$

For $H_0(\mathrm{div}, \Omega)$, we start by defining the space RT_0 of the lowest-order Raviart-Thomas elements on a single, regular hexahedron T [25], [26]:

$$RT_0(T) = \mathcal{P}_{1,0,0}(T) \times \mathcal{P}_{0,1,0}(T) \times \mathcal{P}_{0,0,1}(T),$$

where $\mathcal{P}_{i,j,k}(T)$ denotes the set of polynomial functions defined on T of degrees i, j, and k in x_1, x_2, and x_3.

$$Aj + B^T u = b \tag{13a}$$

$$Bj = 0, \tag{13b}$$

we can left-multiply A^{-1} to (13a) and solve for j, i.e., $j = A^{-1}(b - B^T u)$. Substituting this representation of j into (13b) leads to

$$\begin{aligned} Bj = BA^{-1}(b - B^T u) &= 0 \\ \Leftrightarrow BA^{-1}B^T u &= BA^{-1}b. \end{aligned} \tag{14}$$

$S = BA^{-1}B^T$ is the so-called *Schur complement*, $m_S = n_s =$ #elements. S is positive semidefinite (if $\ker(B) = \{0\}$ positive definite) and since A is symmetric, also S is symmetric [22]. Thus, with $h = BA^{-1}b$, solving (10) is reduced to solving

$$Su = h. \tag{15}$$

(15) could now be solved using the (conjugated) Uzawa-iteration [22], [24], [36].

[Vorwerk, Engwer, Pursiainen & Wolters, *IEEE Trans Med Imag, 2017*]

Comparing mixed FEM and CG-FEM for EEG

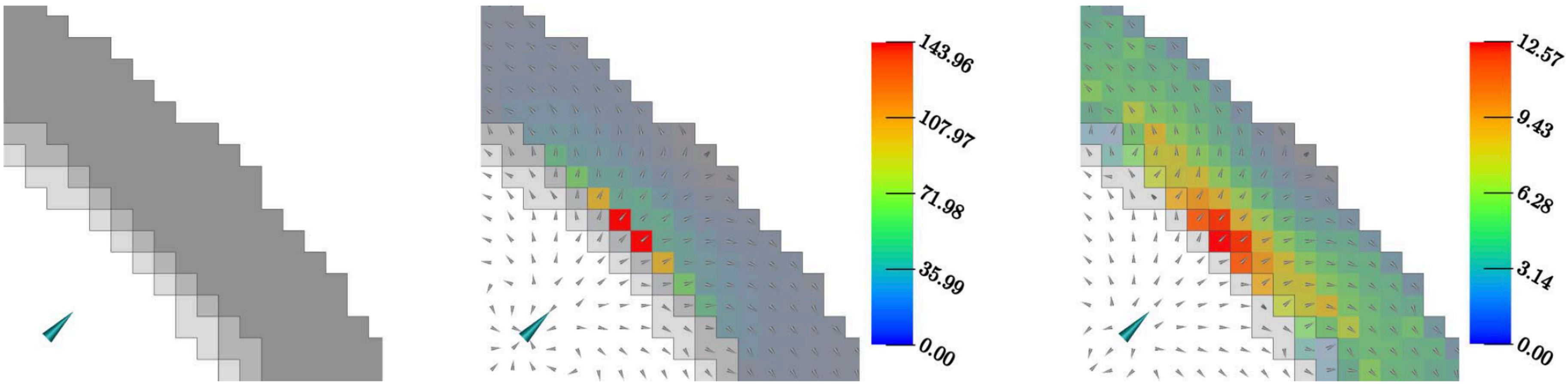

Fig. 7. Geometry of leaky four-layer sphere model (left, compartments from in- to outside/bottom left to top right are brain, CSF, skull, skin, and air) and visualization of strength (only skull and skin, in $\mu A/mm^2$) and direction of volume currents for CG-FEM (middle) and Mixed-FEM simulation (right).

[Vorwerk, Engwer, Pursiainen & Wolters, *IEEE Trans Med Imag, 2017*]

Comparing mixed FEM and CG-FEM for EEG

TABLE III

REALISTIC HEAD MODEL PARAMETERS

	Mesh width (h)	#vertices	#elements	#faces
6C_hex_1mm	1 mm	3,965,968	3,871,029	11,707,401
6C_hex_2mm	2 mm	508,412	484,532	1,477,164
6C_tet_hr	–	2,242,186	14,223,508	27,314,610

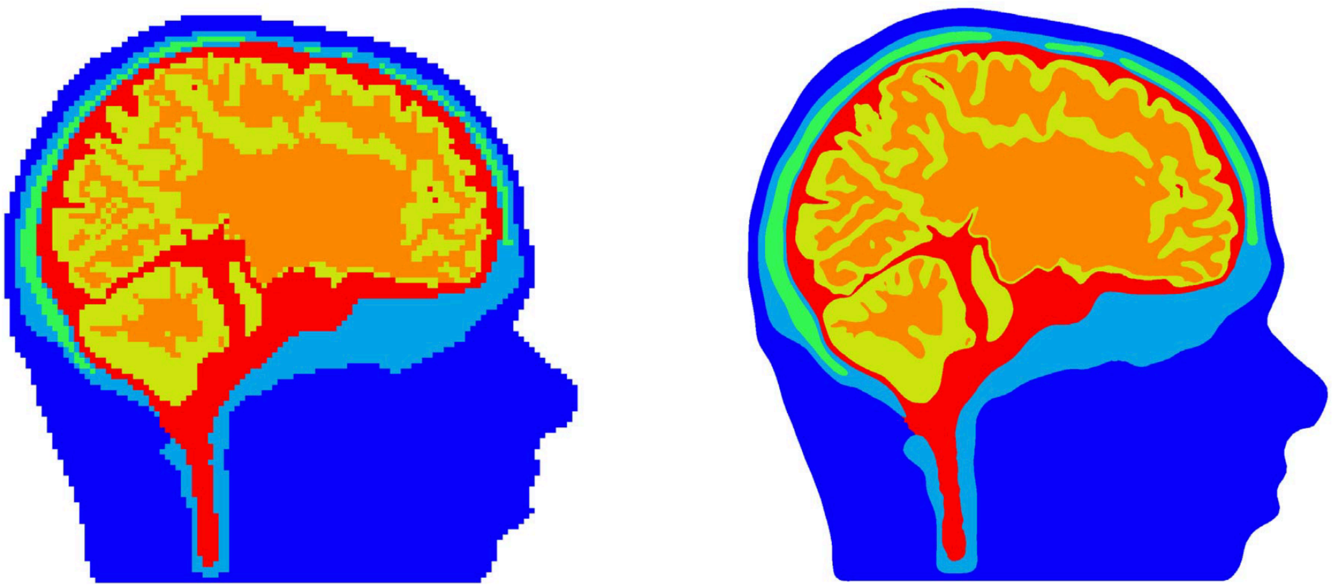

Fig. 3. Visualization of realistic six-compartment hexahedral (*6C_hex_2mm*, left) and high-resolution reference head model (*6C_tet_hr*, right).

[Vorwerk, Engwer, Pursiainen & Wolters, *IEEE Trans Med Imag, 2017*]

Comparing mixed FEM and CG-FEM for EEG

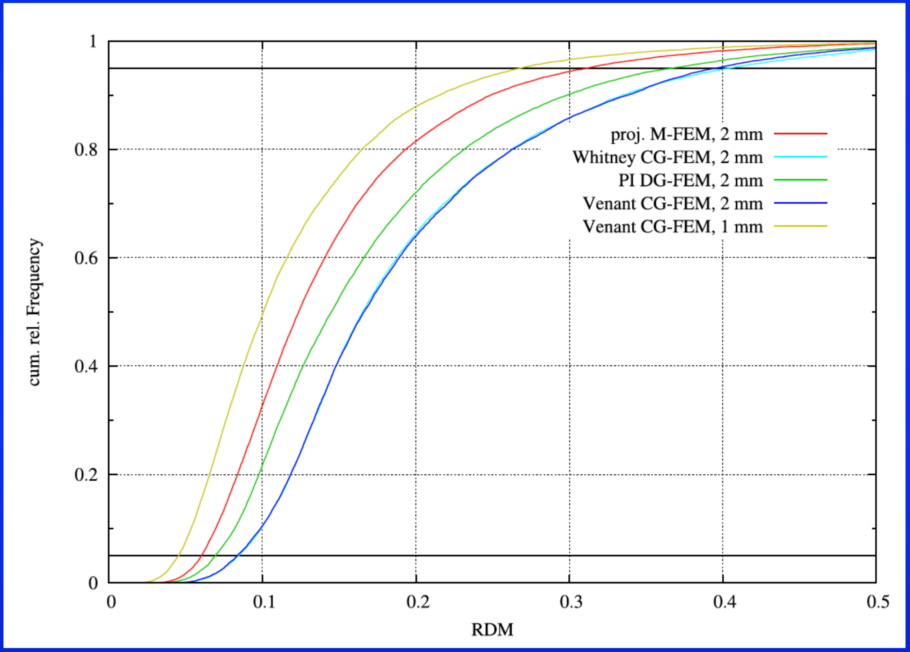

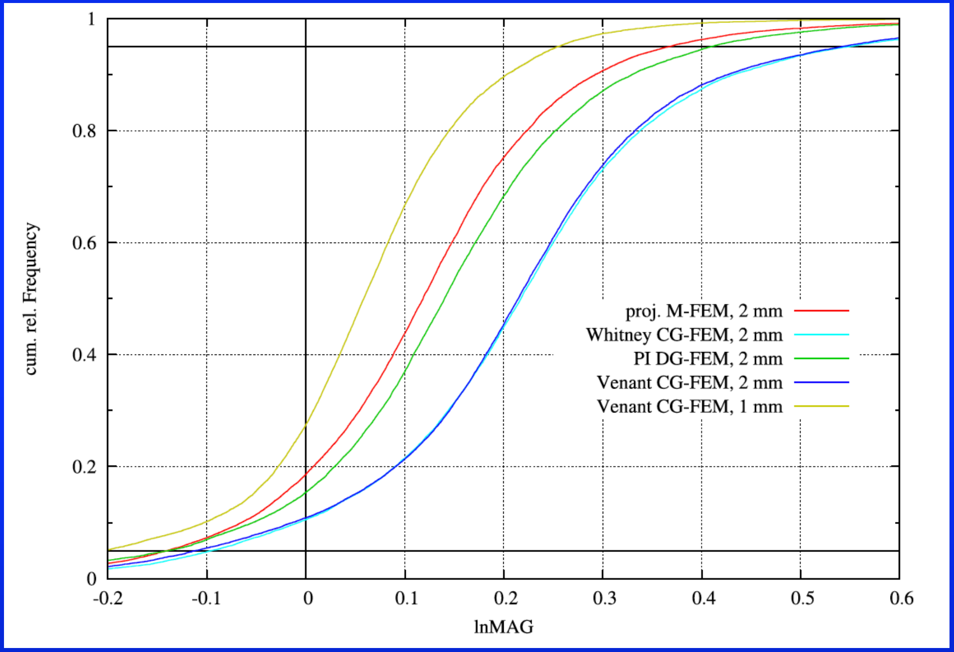

Fig. 8. Cumulative relative errors of RDM (top) and lnMAG (bottom) for EEG in realistic six-layer head model. The horizontal lines indicate the 5th and 95th percentile (lower and upper lines, respectively).

Summary

- BEM forward approaches In 3-compartment headmodels are the current standard, but FEM models allow inclusion of further inhomogeneity or anisotropy, which might be important (-> talk of Maria Carla Piastra)
- Different FEM approaches are available in DUNEuro and it is intructive in applications to check sensitivity to different forward approaches
- Fitted (CG- or DG-FEM) and unfitted FEM (UDG or CutFEM) show accurate results, their choice should mainly depend on the mesh properties
- While mixed FEM and DG-FEM are "current preserving", CG-FEM is not, but this seems only relevant, if thin compartments with considerably different conductivities have to be modeled with limited resolution
- Unfitted FEM, especially CutFEM
    - showed less deviation in the 3-layer/4-layer test case scenarioand thus facilitates modeling of "touching skull and brain surfaces" and might thus facilitate mesh generation
    - outperformed CG-FEM in most categories for both EEG and tDCS
    - needs less degrees of freedom and thus less memory
    - is more expensive for matrix setup (which has to be done only once)

Future outlook: Project PerEpi (funded by ERA PerMed)

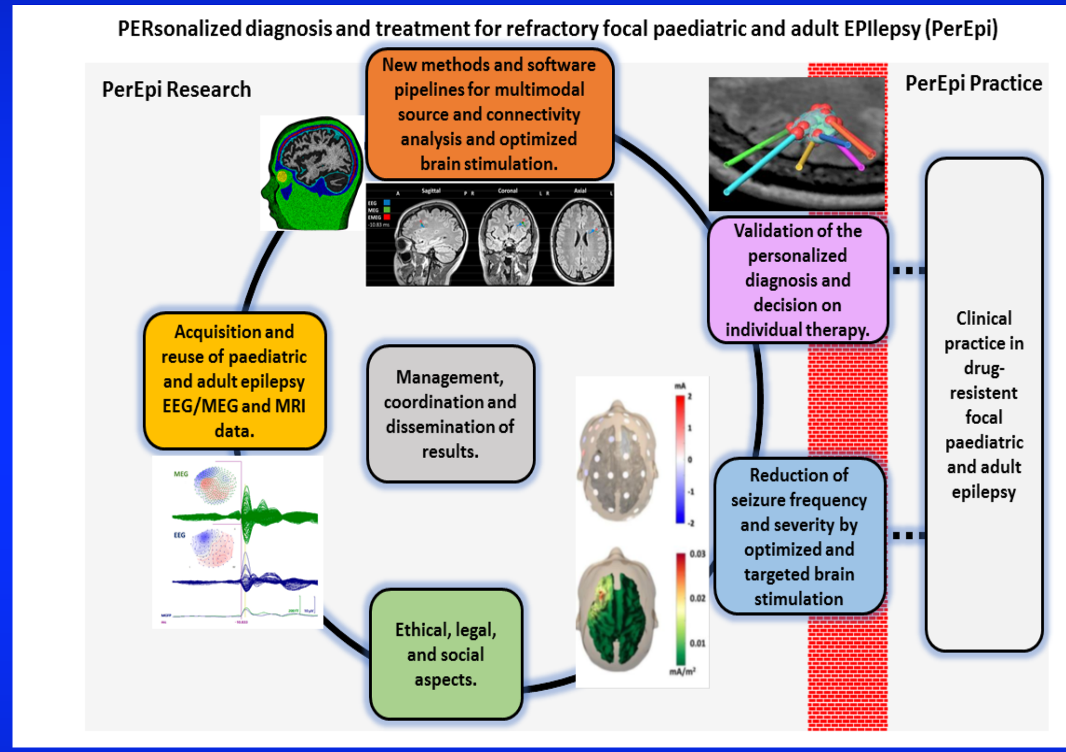

Coordinator:

Prof. Dr. Carsten H. Wolters, Institut für Biomagnetismus und Biosignalanalyse, Westfälische Wilhelms-Universität Münster

Principal Investigators:

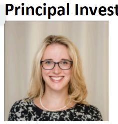

Prof. Dr. Alena Buyx, Institut für Geschichte und Ethik der Medizin, Technische Universität München

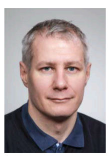

Prof. Dr. Sampsa Pursiainen, Computing Sciences, Tampere University, Tampere, Finland

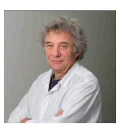

Prof. Dr. Fabrice Wallois, Inserm U 1105, GRAMFC, Universite de Picardie Jules Verne, Amiens, Frankreich






Thank you for your attention!

DFG

DAAD

NIH

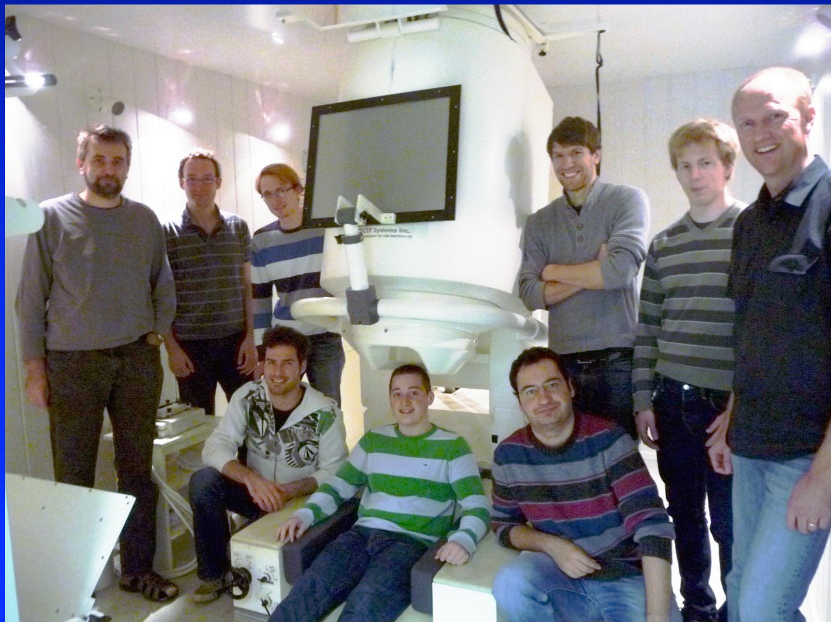

2010-2016

DUNEuro

Since 2016

Münster SIM-NEURO workgroup